

MODELING EVOLUTION AND DISSEMINATION OF RESISTANCE  
UNDER TEMPORALLY CHANGING ANTIMICROBIAL CONCENTRATION

by

Dilara Selin Kubilay

B.Sc. in Chemistry, Boğaziçi University, 2016

Submitted to the Institute of Environmental Sciences in partial fulfillment of  
the requirements for the degree of  
Master of Science  
in  
Environmental Sciences

Boğaziçi University

2018

To my dearest mother and father,

## ACKNOWLEDGEMENTS

I would like to sincerely thank my advisor Assist. Prof. Ulaş Tezel for his guidance and extensive knowledge which helped me move forward throughout this thesis work. His patience, support and encouragement showed me how competent work in science is achieved. I would also like to thank my thesis committee members, Prof. Dr. Ali Kerem Saysel and Assoc. Prof. Dr. A. Evren Tuğtaş Karnabat for the time and knowledge they shared to evaluate this thesis.

I would like to thank my lab mate Seyedmehdi Emadian for his motivational and supportive friendship. He was there for me whenever I got lost in the dark corners. I would also like to thank Enre Karakaya for his cooperative research understanding as he helped me immensely in weekend errands. I would like to especially thank my colleagues and friends, Begüm Şepitçi, Göksu Çelik, Berivan Ülger and Elif Şahin for their friendship throughout my graduate years. Finally, Mete deserves a special mention due to his continuous encouragement and support which cannot be overstated.

I would also like to thank my father, Ersun Kubilay, for being there for me and for showing me that science sometimes requires wetting the hands instead of contemplating a way out. I would also like to thank my mother, Pınar Kubilay, for her curiosity and support and for her patience in keeping me company late at night and at weekend lab works. I would also like to thank my brother, Ekin, for his practical solutions and exemplary cool attitude when facing a difficulty. Finally, I would like to express my gratitude to my inspirational aunt Prof. Dr. Nilsun İnce and my uncle Mehmet Ali İnce for their infinite support and motivation which helped me carry on.

Throughout my graduate studies, I was financially supported by TÜBİTAK 2210-E Graduate Scholarship Program, thus completion of this thesis is partially supported by TÜBİTAK.

## ABSTRACT

### MODELING EVOLUTION AND DISSEMINATION OF RESISTANCE UNDER TEMPORALLY CHANGING ANTIMICROBIAL CONCENTRATION

Quaternary ammonium compounds (QACs) are one of the most extensively used cationic biocides in human and animal health care facilities. Along with their many advantages as an antimicrobial agent, one of their biggest disadvantage is that QACs may facilitate development of antimicrobial resistance in bacteria which also promote antibiotic resistance at sub-inhibitory concentrations. Since QACs are biodegradable biocides, their concentrations may decrease substantially after they are applied to surfaces in hospitals. Thus, biodegradation creates environments with QACs at sub-inhibitory concentrations which are hotspots for evolution of QAC resistance. The objective of this study was to elucidate the role of biodegradation on the development of resistance to benzalkonium chlorides (BACs), one of the most extensively used group of QACs, by a BAC susceptible microorganism when a BAC degrader is present. *Pseudomonas* sp. BIOMIG1 and a strain of *E. coli* were used as BAC degrader and BAC susceptible model organisms, respectively, in the experiments. *E. coli* growth was observed above the minimum inhibitory concentrations of BAC when BIOMIG1 was present in the medium. Furthermore, *E. coli*'s BAC resistance increased when this co-culture system was operated in a continuous reactor. Additionally, a model that simulates the dynamics of interactions in such a microbial community was developed, calibrated and verified successfully with the experimental data. Outcomes of this study may be useful to further explore processes involved in the evolution and dissemination of antimicrobial resistance in microbial communities in human health related environments.

## ÖZET

### ZAMANLA DEĞİŞEN ANTIMİKROBİYAL KONSANTRASYONU ALTINDA DİRENÇ OLUŞUMUNUN VE YAYILIMININ MODELLENMESİ

Dördüncül amonyum bileşikleri(DABlar) insan ve hayvan sağlık merkezlerinde en çok kullanılan katyonik yüzeyaktif dezenfektanlardandır. Yüksek kullanım oranlarına rağmen minimum inhibisyon konsantrasyonunun altındayken mikroorganizmalarda antimikrobiyal direncinin yaydıkları tespit edilmiştir. Yayılan antimikrobiyal direnci ise antibiyotik direncini tetiklemektedir. DABlar biyolojik olarak parçalanabilirler. Bu nedenle hastahane yüzey alanlarında kullanımlarını takiben konsantrasyonları minimum inhibisyon konsantrasyonunun altına düşmektedir ve dolayısıyla DAB direncinin yayılımı kolaylaşmaktadır. Bu çalışmanın amacı en yaygın kullanılan DABlardan olan benzalkonyum klorürlerin (BAK) biyolojik degradasyonunun, antimikrobiyal direncinin yayılmasına katkısı belirlemektir. BAK a duyarlı ve BAK a dirençli iki mikroorganizma sürekli ve kesikli deney mekanizmalarında gözlemlenmiş ve BAK direncinin yayılımını simüle eden bir model hazırlanmıştır. Deneylerde BAK'a dirençli mikroorganizma olarak *Pseudomonas* sp. BIOMIG1 suşu, BAK'a duyarlı mikroorganizma olarak ise *E. coli* kullanılmıştır. Deney sonuçlarında *E. Koli*'nin BIOMIG1 ile aynı ortama konulduğu zaman, normal şartlarda büyümesini engelleyen DAB konsantrasyonun üzerinde büyüebildiği tespit edilmiştir. Aynı sistem sürekli bir deney mekanizmasında işletildiğinde ise *E. Koli*'nin direncinde bir artma gözlemlenmiştir. Tüm bu deney sonuçları kullanılarak yeni bir model geliştirilmiş, kalibre edilmiş ve doğrulanmıştır. Bu çalışmadan elde edilen veriler ile insan sağlığıyla ilişkili ortamlarda, antimikrobiyal direnci oluşumu ve yayılımı ve geçirdiği proseslerle ilgili araştırmalara katkıda bulunmak amaçlanmıştır.

## TABLE OF CONTENTS

ACKNOWLEDGEMENTS.....	iv
ABSTRACT.....	v
ÖZET.....	vi
TABLE OF CONTENTS.....	vii
LIST OF FIGURES.....	ix
LIST OF TABLES.....	xi
LIST OF SYMBOLS/ABBREVIATIONS .....	xii
1. INTRODUCTION.....	1
1.1. Antimicrobials.....	1
1.2. Resistance Mechanisms.....	2
1.3. Resistance Evolution Mechanisms.....	4
1.4. Sub-inhibitory Concentration.....	6
1.5. Modeling Resistance.....	8
2. OBJECTIVES.....	12
3. APPROACH.....	17
4. MATERIALS AND METHODS.....	18
4.1. Chemicals.....	18
4.2. Microorganisms.....	19
4.2.1. Bacteria Strains Used in the Experiments.....	19
4.2.2. Preparation of Cultures.....	19
4.3. Characterization of <i>E. coli</i> .....	19
4.3.1. BAC Inhibition Assays.....	19
4.3.1.1. In Liquid Medium.....	19
4.3.1.2. On Agar Plates.....	20
4.4. Batch Experiments.....	20
4.4.1. <i>E. coli</i> in Maltose.....	20
4.4.2. <i>Pseudomonas sp.</i> BIOMIG1 in BAC.....	21
4.4.3. <i>E. coli</i> in Maltose and BAC.....	21
4.4.4. <i>E. coli</i> and <i>Pseudomonas sp.</i> BIOMIG1 in Maltose and BAC.....	21
4.5. Continuous Flow Experiments.....	22
4.5.1. <i>E. coli</i> in Maltose.....	22

4.5.2. <i>P. sp.</i> BIOMIG1 in BAC.....	23
4.5.3. <i>E. coli</i> and <i>P. sp.</i> BIOMIG1 in Maltose and BAC.....	24
4.6. Media, Broth and Agar Plates.....	24
4.6.1. Luria Bertani (LB) Broth.....	24
4.6.2. LB-BAC Broth.....	24
4.6.3. Mineral Salt Medium (M9) .....	24
4.6.1. Plates.....	25
4.6.1.1. LB Agar Plates.....	25
4.6.1.2. LB-BAC Plates.....	25
4.6.1.3. LB-HiBAC Plates.....	25
4.6.1.4. CHROM™Agar ECC Agar Plates.....	26
4.6.1.5. CHROM®Agar Pseudomonas™ Plates.....	26
4.6.2. 0.85 % Saline Solution.....	26
4.6.3. BACs Stock Solution.....	26
4.6.4. C14BDMA-Cl Stock Solution.....	26
4.6.5. Maltose Stock Solution.....	26
4.7. Analytical Methods.....	27
4.7.1. BAC Analysis.....	27
5. MODEL STRUCTURE AND EQUATIONS.....	29
5.1. System Description.....	29
5.2. Model Processes.....	29
5.3. Model Equations.....	30
5.4. Baseline Values and Data Interpretations.....	32
5.5. Estimating the Parameter Values from the Experimental Data.....	34
6. RESULTS & DISCUSSION.....	37
6.1. Characterization of <i>E. coli</i> .....	37
6.2. Model Calibration.....	38
6.2.1. BAC Degradation in Batch Reactors by <i>Pseudomonas sp.</i> BIOMIG1.....	38
6.2.2. Maltose Degradation in Batch Reactors by <i>E. coli</i> .....	39
6.2.3. Growth Dynamics of the Co-culture Batch Reactor under BAC Stress.....	40
6.3. Model Verification and Simulations.....	43
6.4. Simulations to Identify Resistance Promoting Conditions.....	46
7. CONCLUSIONS.....	53
REFERENCES.....	55
APPENDIX.....	61

## LIST OF FIGURES

Figure 1.1. The action of antimicrobial agents and target site mutation as a resistance mechanism. ....	3
Figure 2.1. Structure of quaternary ammonium compounds ( $R_n$ 's are functional groups and X is a halide). ....	12
Figure 2.2. General structures of QAC subgroups. ....	13
Figure 4.1. Chemical structure of (A) $C_{12}$ BDMA-Cl, (B) $C_{14}$ BDMA-Cl, (C) $C_{16}$ BDMA-Cl .....	18
Figure 4.2. Chemical structure of maltose .....	18
Figure 4.3. An illustration of the continuous-flow reactor system.....	22
Figure 4.4. Picture of the continuous-flow reactor system .....	23
Figure 4.5. Representative HPLC chromatogram of $C_{12}$ BDMA-Cl in red, $C_{14}$ BDMA-Cl in blue and $C_{16}$ BDMA-Cl in green.....	27
Figure 4.6. Calibration curves of $C_{12}$ BDMA-Cl, $C_{14}$ BDMA-Cl and $C_{16}$ BDMA-Cl.....	28
Figure 5.1. Biological processes in the model system .....	29
Figure 5.2. The experimental and the modelling processes .....	35
Figure 6.1. Optical density in tubes containing maltose and inoculated with <i>E. coli</i> between 2 and 1024 mg/L BAC concentration .....	37
Figure 6.2. Profile of (A) BAC degradation and (B) BIOMIG1 growth in a batch reactor. Lines represent model simulations with different set of parameter values.....	39

Figure 6.3. Profile of (A) maltose degradation and (B) <i>E. coli</i> growth in a batch reactor. Lines represent model simulations with different set of parameter values.....	40
Figure 6.4. Profile of (A) BAC utilization and (B) BIOMIG1 growth in the co-culture batch reactor. Solid line represents model simulations of the variables $S_{BAC}$ and $X_{Ps}$ . .....	41
Figure 6.5. Profile of (A) predicted maltose utilization, (B) susceptible and (C) resistant <i>E. coli</i> growth in the co-culture batch reactor. Solid line represents model simulations of the variables $S_{Malt}$ and $X_{Ec}^S$ and $X_{Ec}^R$ .....	43
Figure 6.6. Profile of (A) BAC utilization and (B) BIOMIG1 growth in a continuous flow reactor. Solid line represents model simulations of the variables $S_{BAC}$ and $X_{Ps}$ . .....	44
Figure 6.7. Profile of (A) predicted maltose utilization, (B) susceptible and (C) resistant <i>E. coli</i> growth in a continuous flow reactor. Solid line represents model simulations of the variables $S_{Malt}$ and $X_{Ec}^S$ and $X_{Ec}^R$ .....	45
Figure 6.8. Simulations of different BAC concentrations.....	48
Figure 6.9. Simulations for different Q values.....	49
Figure 6.10. (A) Maltose concentration, (B) <i>E. coli</i> <sup>Sus</sup> concentration and (C) <i>E. coli</i> <sup>Res</sup> concentration when BAC is fixed at 21 $\mu$ M (8 mg/L) and the BIOMIG1 concentration is 0. ....	50
Figure 6.11. (A) Maltose concentration, (B) <i>E. coli</i> <sup>Sus</sup> concentration and (C) <i>E. coli</i> <sup>Res</sup> concentration when BAC is fixed at 43 $\mu$ M (8 mg/L) and the BIOMIG1 concentration is 0. ....	51

## LIST OF TABLES

Table 2.1. The specific efflux pumps and their effect on various antimicrobial agents .....	16
Table 4.1. The contents of the solutions.....	20
Table 4.2. Chemical composition of LB Broth. ....	24
Table 4.3. Composition of M9 medium .....	25
Table 4.4. Composition of the trace metal stock solution.....	25
Table 5.1. Definitions of the parameters used in the model equations .....	30
Table 5.2. Literature values for BOD based substrate utilization and growth kinetics constants..	33
Table 5.3. Conversion factors used to synchronize units of literature values with model units ....	33
Table 5.4. Baseline values of growth parameters calculated based on literature values.....	33
Table 5.5. Other parameters, constants and initial values .....	34
Table 5.6. The experiment used for each fitted parameter .....	35
Table 6.1. Fixed parameters of the batch co-culture <i>E. coli</i> and BIOMIG1 experiment .....	42
Table 6.2. Fixed parameters of the continuous co-culture <i>E. coli</i> and BIOMIG1 experiment .....	46

## LIST OF SYMBOLS/ABBREVIATIONS

Symbol	Explanation	Units Used
Q	Flow Rate	mL/hr
D	Dilution Rate	hr <sup>-1</sup>
V	Volume	mL
R	Functional group	
S <sub>Malt</sub>	Concentration of Maltose	μM
S <sub>BAC</sub>	Concentration of BAC	μM
X <sub>P<sub>s</sub></sub>	<i>Pseudomonas</i> concentration	cell/L
X <sub>E<sub>c</sub></sub>	<i>E. coli</i> concentration	cell/L
Y <sub>BAC</sub>	Cell yield dependent on the BAC	cell/μM S <sub>i</sub>
Y <sub>Malt</sub>	Cell yield dependent on the Malt	cell/μM S <sub>i</sub>
k <sub>BAC</sub>	Maximum degradation rate constant of BAC	μmol/hr*cell
k <sub>Malt</sub>	Maximum degradation rate constant of Malt	μmol/hr*cell
k <sub>d</sub>	Decay rate constant for cells	hr <sup>-1</sup>
M <sub>Malt</sub>	Half saturation coefficient of Maltose	μM
M <sub>BAC</sub>	Half saturation coefficient of BAC	μM
μ	Growth rate	hr <sup>-1</sup>
μ <sub>Max</sub>	Maximum growth Rate	hr <sup>-1</sup>
C12BDMA-Cl	Dodecyl benzyl dimethyl ammonium chloride	
C14BDMA-Cl	Tetradecyl benzyl dimethyl ammonium chloride	
C16BDMA-Cl	Hexadecyl benzyl dimethyl ammonium chloride	
MIC	Minimum inhibition concentration	μM

Abbreviation	Explanation
QAC	Quaternary Ammonium Compounds
BAC	Benzalkonium Chlorides
U.S. EPA	U.S. Environmental Protection Agency
HPLC	High Pressure Liquid Chromatography
MPC	Mutant prevention Window
DNA	Deoxyribo Nucleic Acid

LB	Luria Bertani broth
M9	Mineral salt medium
UV/Vis	Ultraviolet-Visible

## 1. INTRODUCTION

### 1.1. Antimicrobials

“Antimicrobial agent” is a broad term used to describe the group of chemical substances used to kill or inhibit the growth of microorganisms. It is generally divided in two sub-groups: the –cidals and the –statics. The suffix –cidal is used for substances which kill the microorganism, such as bacteriocidals or fungicidals. The suffix –static is used for the growth inhibitors which do not kill the bacteria, such as bacteriostatic or fungistatic agents (Madigan, et al., 2003). Disinfectants, which are among the most common antimicrobial agents, are bacteriocidals used on surfaces to kill the living microorganisms on the surface. Antibiotics are biocides used within the body, while antiseptics are those applied on living tissues (Carmona-Ribeiro, et al., 2013).

The word “antibiotic”, first introduced by S. A. Waksman, was originally used for the low molecular secondary metabolites of bacteria and fungi that inhibit the growth of other microorganisms at low concentrations. Although it is not certain why bacteria produce antibiotics, it is suspected that the main driving force behind the antibiotic production is to eliminate susceptible microorganisms from the resource competition (Madigan, et al., 2003).

There is historic evidence that even modern-like antibiotics had been used in ancient Nubia and in Egypt throughout Roman occupation (1<sup>st</sup> century), though they were not as available as they are nowadays (Gauld, 2016). Even though covering the infected area with *Penicillium* mold to inhibit bacterial growth was a common practice in late 19<sup>th</sup> century, it was Alexander Fleming who made antibiotics famous (Russell, 2002). Introduction of this new group of chemicals by the end of 1930s was a revolution in fighting against microbial infections and antibiotics still save millions of lives today.

Quaternary ammonium compounds (QACs) which are bacteriocidal agents used for disinfecting the surfaces in hospitals and homes are introduced into the market concurrently with penicillin (Gerba, 2015). QACs are being used for hygienic purposes almost for a century now and sold uncontrollably as opposed to antibiotics (Russell, 2003). QACs are among the high production chemicals and their consumption exceeds a million tonnes worldwide annually.

As the use of antibiotics increased, bacteria resistant to them started to emerge since World War II (Ventola, 2015). Penicillin, which is a naturally occurring substance, is the first antibiotic that bacteria developed resistance to. Although resistance to a natural antibiotic is expected, many bacteria develop resistance to synthetic antibiotics as well. Therefore, rate of administration and use is another factor that regulates the proliferation of resistance in the environment. Many studies showed that there is a direct correlation between clinical introduction of an antibiotic and resistance to it in the pathogens they are used for (Allen, et al., 2010).

While antibiotic resistance was under the spot not long after the prescription of penicillin in 1940s, QAC resistance gained interest around 1980s (Russell, 2002). Co-occurrence of resistance to antibiotics and QACs, in bacteria, suggests that there may be a link between them. In spite of today's restricted consumption of antibiotics, the uncontrolled use of QACs may have a similar effect in dissemination of resistant strains.

## **1.2. Resistance Mechanisms**

Antibacterial agents are divided into 3 groups depending on their effects on bacteria: bacteriostatic, bacteriocidal, and bacteriolytic. Bacteriostatic agents do not kill the bacteria but inhibit their growth, so the total cell count and the viable cell count remains constant following their application. Bacteriocidal agents kill cells, therefore the viable cell count decreases but the total cell count remains constant as the dead cells are not destroyed. Contrarily, bacteriolytic agents kill the bacteria and destroy the cell thus, both the viable cell count and the total cell count decreases. For this reason, the action an antimicrobial agent mostly depends on the class of the agent. Bacteriostatic antibiotics, such as sulfonamides, interfere with the protein synthesis by binding to the ribosomes. But when they are removed from the environment, the agent releases the ribosome and the growth continues. Contrary to this, bacteriocidal and bacteriolytic antibiotics bind firmly to their target and even when the concentration of the agent is decreased, the bond between the agent and the target is never broken thus the cells never continue to grow. Furthermore, bacteriolytics such as penicillin inhibit the peptidoglycan cell wall production and at the same time triggers the production of an enzyme called autolysin which degrades the cell itself. This then results in the self-destruction of the cell (Madigan, et al., 2003).

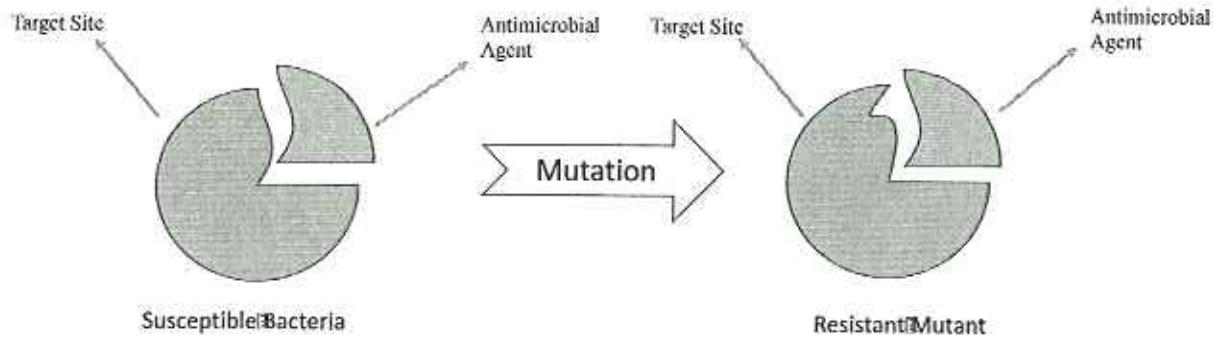


Figure 1.1. The action of antimicrobial agents and target site mutation as a resistance mechanism.

In the 1900s, Paul Ehrlich defined the concept of selective toxicity as the ability of an antimicrobial agent to inhibit through specific target sites. Thus, only the cells containing that target site are adversely effected by the compound. The agent binds to a specific target just as in the key-lock concept (Figure 1.1). When an antimicrobial agent encounters with its target, it binds to it only if they match. For this reason, the modification of the target site is a strong resistance as it is rarely reversible and inhibits the antimicrobial action altogether. The target site of an agent may be the outer cell components, cytoplasmic membrane or cytoplasmic components. Cationic biocides, for example, alter the hydrophobicity of the outer cell and let themselves in. Only then, they interact with their cytoplasmic target (Maillard, 2002). The spectrum of the agent is also determined by how specific the target is. Broad spectrum antibiotics such as sulfonamide fit to both gram positive and gram negative bacteria, while penicillin effect only gram positive bacteria (Madigan, et al., 2003). Biocides on the other hand have low target specificity; they have one or more target sites within the cell. As a result, biocides have a broader spectrum of activity and may inhibit the vast majority of bacteria at once (Gilbert, et al., 2003).

Antimicrobial agents can also be classified more specifically based on their mode of action. They may act as an inhibitor of: (1) cell wall synthesis, (2) cell membrane function, (3) protein synthesis, (4) nucleic acid synthesis or (5) other metabolic processes (Kohanski, et al., 2010; Gilbert, et al., 1985) QACs, for example, disturb the lipid bilayers of the outer membrane by an attack of the positively charged quaternary nitrogen to the head of the acidic phospholipids. Then, the micelle form of QACs solubilize the membrane with hydrophobic tails and the cell dies due to the leakage of the cytoplasmic materials (McBain, et al., 2004). Contrarily, chlorine-releasing agents, which are widely used hard-surface disinfectants, inhibit growth by interfering the cellular protein production in the cell. More precisely, they directly target the DNA synthesis by oxidizing the nucleotides (McDonnell, et al., 1999; McKenna, et al., 1988).

A strain is said to be resistant to a biocide when it's not killed at the advised application concentration. Microorganisms can tolerate antibiotics and biocides through various mechanisms. Increasing the efflux, reducing the cellular permeability, changing the antibiotic target site by mutation, changing or overproducing the target site, degrading the antimicrobial agent and biofilm formation are the most common mechanism that are encountered (Russell, 2002b; Miao, et al., 2012). Every organism has a specific outer layer in terms of composition and permeability. A thick membrane or a reduced permeability prevents the biocide from entering the cell (McDonnell, et al., 1999). The natural ineffectiveness of penicillin on gram negative bacteria, for example, comes from its impermeable cell wall (Madigan, et al., 2003). Some other mechanisms are; a mutation which modifies the target site and prevents the biocide from binding to it (as in Figure 1.1), and the degradation of the antimicrobial agent which enables the bacteria to survive by decreasing the concentration to a non-inhibiting level (Allen, et al., 2010; Blair, et al., 2015; Cantón, et al., 2011).

Among these mechanisms, overexpression of the efflux pumps is of great importance because there is evidence that most antimicrobial agents succeed in penetrating gram-negative bacteria, but are thrown out by efflux pumps before reaching their target (Aleksun and Levy, 2007). These pumps serve as a discharge for the unwanted substances in the cell (Cloete, 2003). Increasing the number of pumps accelerates the rate of transport of the substance outside the cell membrane. By nature, efflux pumps have a broad spectrum of effectiveness. They enable bacteria to tolerate multiple biocides therefore they are also called multidrug efflux pumps. For instance, AcrAB-TolC can act on QACs, triclosan, chlorhexidine, ampicillin, chloramphenicol, nalidixic acid, tetracycline and rifampicin. (Gilbert, et al., 2003) These pumps may be chromosomally encoded and their expression may be increased at different conditions. They may also be acquired through mobile genetic elements (Tezel, et al., 2015). Acquiring resistance to QACs, for instance, is relatively easy as the "*qacA*" gene which encodes multidrug efflux pumps can be found on a multi-resistance plasmid (Gilbert, et al., 2003).

### 1.3. Resistance Evolution Mechanisms

Resistance can be divide into three main sub-groups: intrinsic, acquired and adaptive. Intrinsic resistance is the natural form of resistance which has been developed gradually by the bacterial strain as it is exposed to natural biocides and toxicants at the natural background levels (Fernandez, et al., 2012). Acquired resistance is a fast process of adaption to a stress condition, generally through gene transfer or mutations (Fernandez, et al., 2012; Allen, et al., 2010). The frequency of mutations to occur is relatively low and ranges between  $10^{-9}$  to  $10^{-7}$  during the duplication of the

genetic material (Focks, 2005). Random mutations that emerges a new resistance gene are very rare, although not impossible. But, selective pressure of an antimicrobial agent in the environment can increase the frequency of such mutations. Furthermore, the mutant which has a selective advantage due to the new modification will be favored over the susceptible microorganism and thus, proliferate. But, it is also expected that these mutations have a fitness cost and that wild strains are favored over mutants when the selective pressure is removed. Mutations such as the modification of the target of the antimicrobial agent may remain in the cell if this change does not have a cost and accordingly, does not cause a disadvantage to the cell in the absence of the antimicrobial agent. When this is the case, the resistance increases even more. But, some other mutations, such as the overexpression of efflux pumps, have a cost and are reversed when the antimicrobial agent is removed from the environment. Therefore, overexpression of efflux pumps results in a relatively small shift in the MIC level of the antimicrobial agent compared to the shift caused by the modification of the antimicrobial target site since the latter has a lower fitness cost than the former (Focks, 2005).

Another resistance acquisition mechanism is the horizontal gene transfer. Horizontal gene transfer is the transfer of genetic material from one cell to another by mechanisms other than inheritance, which is referred to as vertical gene transfer (Madigan, et al., 2003). Most of the resistance mechanisms can be transferred horizontally with mobile genetic elements such as integrons, transposons or plasmids (Wright, 2012). This can occur between strains as well as between species and genera, and accelerates the dissemination of resistance faster than mutational or adaptive resistance (Roberts, 2012). Contrary to mutational resistance, which results in a small decrease in susceptibility, horizontal gene transfer favors a higher level of tolerance (Fernandez, et al., 2012). Genes are transferred laterally in three ways: (1) Conjugation which is a transfer of small pieces of DNA i.e. plasmids within closely related bacteria via direct cell-to-cell contact; (2) Transformation which is the acquisition of a piece of DNA present in the external environment by bacteria, and (3) Transduction which is the transfer of DNA between two closely related bacteria via a common bacteriophage (Allen, et al., 2010).

Finally, there is the adaptive resistance. This type of resistance is triggered by environmental conditions and occurs rather slowly, just as in mutational resistance. Although the mechanisms are not clearly known, adaptive resistance is developed in bacteria exposed to gradually increasing stress factor starting from the sub-inhibitory level. It is also called acclimation. Biofilm formation is one of the mechanisms that promote adaptive resistance. Resistance acquired by adaptive processes can be lost when the stress disappears (Fernandez, et al., 2012).

Acquired and adaptive resistances are the most frequently detected resistance mechanisms in the medical, domestic and environmental settings. There are three prerequisites for their occurrence: (1) a stressor at sub-inhibitory concentration (2) a domain with a concentration gradient and (3) a resistance gene. Based on these three prerequisites, one of the most favorable route for development and dissemination of resistance occurs as follows: (1) Wastewater from hospitals contain all three of the antibiotics, disinfectants and pathogens. This wastewater is commonly discharged into central wastewater collection systems and goes to wastewater treatment plants; (2) Antibiotics and disinfectants are diluted with domestic wastewater and urban runoff or degraded so that their concentration drops at sub-inhibitory levels for most of the bacteria; (3) wastewater treatment plants harbor a diverse microbial community and genes, including antimicrobial resistance genes; (4) Human originated pathogens interact with bacteria in wastewater treatment microbiome under sub-inhibitory antibiotic and disinfectant concentration and get acclimated to the biocide or acquire resistance genes. Finally, (5) resistant pathogens reach hospitals where they exposed to higher biocide concentrations and where resistance is selected and proliferates (Baquero, et al., 2008; Martinez and Olivares, 2012).

#### 1.4. Sub-inhibitory Concentration

Carrying a bunch of extra genes to become resistant has a fitness cost for bacteria. Therefore, external genetic elements and mutations emerge and persist as long as there is a stressor in the environment. It would only be beneficial in the presence of a selective pressure caused by a biocide. When there is not any antimicrobial pressure in the environment, the susceptible bacteria will outcompete the resistant strains because of the fitness cost of carrying resistance genes. But, when there is an antimicrobial agent in the environment, the susceptible microorganism will be inhibited, while resistant ones thrive due to the lack of competition (Martinez and Olivares, 2012).

All antimicrobial agents have a minimum inhibitory concentration (MIC) below which their effectiveness is significantly reduced. In other words, the differing MIC values of different agents for specific bacteria indicate the resistance level of the bacteria to that agent. For example, the MIC of benzalkonium chloride for *E. coli* is 50 µg/mL while it is 250 µg/mL for *P. aeruginosa* (McDonnell and Russell, 1999). So, *P. aeruginosa* is relatively resistant to benzalkonium chloride, compared to *E. coli*. For this reason, antimicrobial agents' recommended dosages are generally above their MIC values. But, after being consumed and partially metabolized, these substances are mixed with the water and send to wastewater treatment plants. When discharged, they are diluted to below their therapeutic level and their inhibitory effect is substantially decreased. Clinical

environments are of highly risky environments for the development and dissemination of resistance since they both contain biocides, i.e. antibiotics and disinfectants, and bacteria that contain resistance genes (Russell, 2002). Therefore, as biocidal chemicals interact with the resistant bacteria in clinical environments, they also create a selective pressure in the environment which results in resistant strains being selected over the non-resistant ones when the concentration of the biocide drops below the sub-inhibitory level (Kummerer, 2004). Thus, horizontal gene transfer as well as mutational and adaptive resistance is more likely to occur in these environments.

Dissemination of resistance occurs in a certain range of biocide concentration which is called the mutant selection window. Above the MIC, some susceptible bacteria continue to mutate to gain resistance. The limiting concentration where even this mutation is inhibited is called the mutant prevention concentration (MPC). Within this window between MIC and MPS, the resistant bacteria are selected over the susceptible. Below the MIC, resistant mutants exist, but they are not selected over susceptible ones. While above the MPC, none of the susceptible bacteria survive. The mutation window phenomenon can also be applied to horizontal gene transfer. The selective pressure between MIC and MPS would facilitate the transfer of mobile genetic elements between resistant and susceptible bacteria via conjugation (Cantón and Morosini, 2011).

Another important factor is the concentration gradient of the environment. When the concentration is homogenous, the selective window is quite narrow. But, when there is a concentration gradient and the environment is composed of several different concentration compartments, the selective window is relatively wide. Mutation to resistance generally requires several steps. In a homogenous concentration environment, these mutations need to occur in a very short period, but the likelihood of several mutations to occur in this period is quite low. Contrarily, in a heterogeneous concentration environment, the low concentration compartment acts as a sanctuary for the susceptible microorganism and provides time for it to carry out the necessary mutations (Hermsen, et al., 2012).

The hospital environments are accepted as a major source for antibiotic resistant microorganism as they bear below-MIC levels of antibiotics and high concentration and diversity of pathogens. An accepted strategy to cope with these pathogen reservoirs is the application of antiseptics and biocides to surfaces in the hospital environments (Cookson, 2005). QACs are among the most extensively used biocides which are approved to be used in healthcare environments by US-FDA (SCENIIR, 2009). Their application concentration is between 400 to 500 mg/L and never exceeds 1000 mg/L (Tezel, et al., 2015). Paradoxically, clinicians are worried that increase in

biocide use may be a contributing factor in dissemination of resistance mechanisms. The first links of benzalkonium chloride resistance (BAC) to antibiotic resistance dates as early as late 1990s and several researches has been conducted to prove this close relation. An early example to this is the research of Akimitsu et al. who first claimed that oxycillin, an antibiotic of the beta-lactam group, and BAC resistance may be encoded on the same plasmid. Thus, an increase in the BAC consumption may result in an increase in the oxycillin resistance.

### 1.5. Modeling Resistance

Antimicrobial resistance models are an important tool for public health decision makers to understand how the bacteria behave at certain antimicrobial concentrations and to predict the future of resistance at current antimicrobial consumption. Various models have been developed in the past. But in general, antimicrobial resistance models can be divided into three subgroups depending on their scope. The resistance can be studied at the genetic level, at the bacterial population level and at the human population level (Opatowski, et al., 2011). In the genetic level, the evolution of resistance is analyzed and phenomena such as mutation or horizontal gene transfer are modeled. At the bacterial population level, competition and selection of resistant mutants are studied. At the human population level, the focus is the spread of resistance via human contact. Even though all these models are of great importance for the evaluation of resistance, spread and possible control policies, only the bacterial population level models are reviewed here as they are in the scope of this research.

Growth of bacterial populations is composed of four phases; lag phase, exponential growth phase, stationary phase and decay phase. This is generally referred to as a logistic growth although several other sigmoidal models such as Richards or Gompertz are used as well (Zwietering, et al., 1990). Nevertheless, these models are all used to describe the number of microorganisms at a specific time and exclude the consumption of their substrate. In other words, these models show the change in the growth rate ( $\mu$ ): the rate starts with zero, increases until it reaches a maximum called maximum specific growth rate ( $\mu_{max}$ ) and then decreases again to zero until the upper limit of the population is reached (Zwietering, et al., 1990). As bacteria grow exponentially, general expression used for the number of bacteria at time  $t$  is ( $X$ ) and can be expressed in terms of initial cell number ( $X_0$ ) and number of duplications in the specified time ( $n$ ) (**Equation 1.1**). Subsequently rate of change of bacteria within time  $t$  can be calculated using **Equation 1.2**.

$$X = X_0 \cdot 2^n \quad (1.1)$$

$$\frac{dX}{dt} = \mu \cdot X \quad (1.2)$$

In a bacterial population, substrate concentration is the major factor that limits growth. Substrate limited growth concept was first introduced by Monod who used the Michaelis-Menten kinetics to express the effect of the changing substrate concentration on the growth rate (**Equations 1.3 and 1.4**). Here,  $\mu$  and  $\mu_{max}$  are the growth rate and maximum growth rate respectively,  $S$  is the substrate concentration and  $K_S$  is the half-saturation constant, also called the “substrate concentration at which the growth rate is half of the maximum growth rate” (Rittmann and McCarty, 2001). The maximum growth rate ( $\mu_{max}$ ) is the growth rate when substrate is not a limiting factor and it decreases as  $S$  decreases.

$$\mu = \mu_{max} \cdot \frac{S}{(K_S + S)} \quad (1.3)$$

$$\frac{dX}{dt} = \mu_{max} \cdot \frac{S}{(K_S + S)} \cdot X \quad (1.4)$$

Substrate is utilized as bacteria grow. Therefore, substrate concentration varies in a microbial population. As a result, bacterial growth equation can be used to express rate of change of substrate in the population using a yield coefficient ( $Y$ ) which is unit mass of cells produced per unit mass of substrate utilized (**Equation 1.5**).

$$\frac{dS}{dt} = -\frac{1}{Y} \cdot \mu_{max} \cdot \frac{S}{(K_S + S)} \cdot X \quad (1.5)$$

When Equations 1.4 and 1.5 solved together, change of substrate concentration and cell density can be simulated at a given initial condition with respect to time. In more realistic models, these equations are developed further by adding other inhibiting or enhancing factors. The cell yield for example is a generalization. In fact, some of the energy from the substrate goes to the maintenance of the cell and other cellular functions such as motility, repair or transfer. Only the leftovers go to the reproduction (Rittmann and McCarty, 2001) and this has been neglected so far in the above equations. Thanks to this partitioning of the energy, the concept of true yield and theoretical yield has been added as can be seen in **Equations 1.6 and 1.7**. Here  $m$  represents the energy that goes to

the maintenance functions of the cell and  $Y_{max}$  denotes the maximum possible cell yield with the remaining energy from the maintenance. From these basic equations, any increasing or decreasing influence on the bacterial growth can be added to the equations with the appropriate sign. Among the most encountered effects, decay effect is added as a subtraction when the equation is used for a long term representation or the predatory effect of protozoa is generally added to the models which represents the soil microbiota (Focks, 2005).

$$\frac{dX}{dt} = \left( \mu_{max} \cdot \frac{S}{(K_S + S)} - m \right) \cdot X \quad (1.6)$$

$$\frac{dS}{dt} = - \frac{1}{Y_{max}} \cdot \mu_{max} \cdot \frac{S}{(K_S + S)} \cdot X \quad (1.7)$$

Bacterial growth kinetics are the starting point of most of the empirical models used in the literature which simulate the dissemination of antimicrobial resistance. Those empirical models integrate additional expressions to the generic growth equations to better simulate the mutation rates, horizontal gene transfer, fitness cost of resistance and competition of resistant bacteria with susceptible ones (Contois, 1959; Madigan, et al., 2003).

A model by Hellweger et al. for example has expressed the dynamics of susceptible and resistant bacteria in a population, as in **Equation 1.8** and **1.9**, where  $X^S$  and  $X^R$  symbolizes the susceptible and resistant bacteria respectively,  $\mu_s$  and  $\mu_R$  are the specific growth rates,  $k_R$  is the specific endogenous respiration rate and  $k_C$  and  $k_S$  are the resistance acquisition and loss rate constants respectively (Hellweger, et al., 2011).

$$\frac{dX^S}{dt} = (\mu_s \cdot X^S) - (k_R \cdot X^S) - (k_C \cdot X^R \cdot X^S) + (k_S \cdot X^R) \quad (1.8)$$

$$\frac{dX^R}{dt} = (\mu_s \cdot X^R) - (k_R \cdot X^R) + (k_C \cdot X^R \cdot X^S) - (k_S \cdot X^R) \quad (1.9)$$

From these equations, the previously mentioned addition and subtraction of desired effects on the bacterial growth can be seen clearly. From the bacterial growth, the energy loss via respiration is subtracted with the  $(k_R X^S)$  term. Moreover, the transformation from susceptible to resistant is expressed with  $(k_C X^R X^S)$ . Finally, the loss of resistance is added to the susceptible bacteria's growth and subtracted from the resistant mutant's growth with the term  $(k_S X^R)$ .

Even though there is a consensus on modeling the bacterial growth kinetics and substrate degradation, mathematical expressions for resistance concepts such as mutation selection window, horizontal gene transfer or inhibitor effect of antibiotics vary a lot. Levin et al., for example, modeled the change in the resistance in a population with the change in the MIC value in a continuous system. Their model assumed that the MIC ( $M$ ) increases with increasing susceptible bacteria density as in **Equation 1.10** within the range of maximum MIC ( $M_{max}$ ) and minimum MIC ( $M_{min}$ ). Here,  $M$  and  $X^S$  denotes MIC and susceptible bacteria density, “ $pd$ ” denotes the density dependent MIC coefficient and “ $k_a$ ” denotes the density at which MIC is half the maximum value (Levin and Udekwa, 2010).

$$M = M_{min} + pd \cdot \left( M_{max} \frac{X^S}{X^S + k_a} \right) \quad (1.10)$$

With the integration of this dynamic MIC value to their growth model, they achieved to simulate three main concepts: (1) the decreasing MIC value with increasing cell density and the inefficacy of the antibiotics at high concentrations of microorganisms, (2) the little change in the resistance with the change in the antibiotic concentration and (3) the drastic effect of the initial bacteria concentration on the resistance level (Levin and Udekwa, 2010).

Another way of expressing the resistance proliferation is to determine a selection rate for the two competitors in the population as in **Equation 1.11**, expressed by Negri et al. in their research on selection of antibiotic resistant strains (Negri, et al., 2000). In this expression,  $r$  represents the resistance selection rate while  $d_{12}$  and  $d_1$  denotes resistant and susceptible strains respectively.

$$r = \ln \left[ \frac{d_{12}(t)}{d_1(t)} \right] - \ln \left[ \frac{d_{12}(0)}{d_1(0)} \right] \quad (1.11)$$

In **Equation 1.11**, resistance is simulated as the difference between the proportion of resistant to susceptible microorganism from the initial proportion. Thus, selection becomes a dynamic variable and the selection window concept can be integrated to bacterial growth kinetics.

## 2. OBJECTIVES

Surface active agents, i.e. surfactants are composed of hydrophobic moieties attached to a hydrophilic head-group. The charge on the hydrophilic group indicates the class of the surfactant as anionic, cationic, non-ionic or amphoteric (McDonnell and Russell, 1999). Quaternary ammonium compounds, so-called QACs or QUATs, are among the most extensively used cationic surfactants. They have been in use for domestic, clinical and industrial applications as surfactants, softeners, disinfectants, preservatives, pesticides and so on since 1930s (Tezel and Pavlostathis, 2011). As the name implies, they are composed of a central nitrogen atom, bonded to four different groups. General notation for QACs is 'R<sub>1</sub>R<sub>2</sub>R<sub>3</sub>R<sub>4</sub>N<sup>+</sup>X<sup>-</sup>' (Figure 2.1) where the R's are functional groups such as hydrogen, methyl, alkyl, benzyl etc. groups while X represents an anion (Hegstad, et al., 2010).

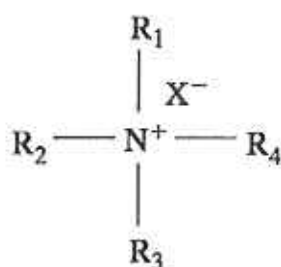


Figure 2.1. Structure of quaternary ammonium compounds (R<sub>n</sub>'s are functional groups and X is a halide) (Tezel and Pavlostathis, 2011).

There are five major subgroups of QACs with respect to the R groups: mono-, di-, benz-, iester- and pyridalkonium halides (Figure 2.2). Among these, benzalkonium chlorides are commonly encountered as a disinfectant in hospitals (Tezel and Pavlostathis, 2011). QACs are formed by a hydrophobic alkyl group attached to a positively charged hydrophilic nitrogen thus they are amphipathic molecules. The antimicrobial activity is facilitated by their positive charge and hydrophobic functional groups which solubilize bacterial cell membrane. Although they cause skin irritation, they are extensively used for cleaning and disinfection purposes on contact surfaces since they are non-toxic to humans (Carmona-Ribeiro, et al., 2013). But lately, they are being disputed over intensely because of their two attributes; their ability to promote resistance in microorganisms (Sidhu, et al., 2002) and their high chemical stability which results in a relatively slow degradation in natural environments (Carmona-Ribeiro, et al., 2006).

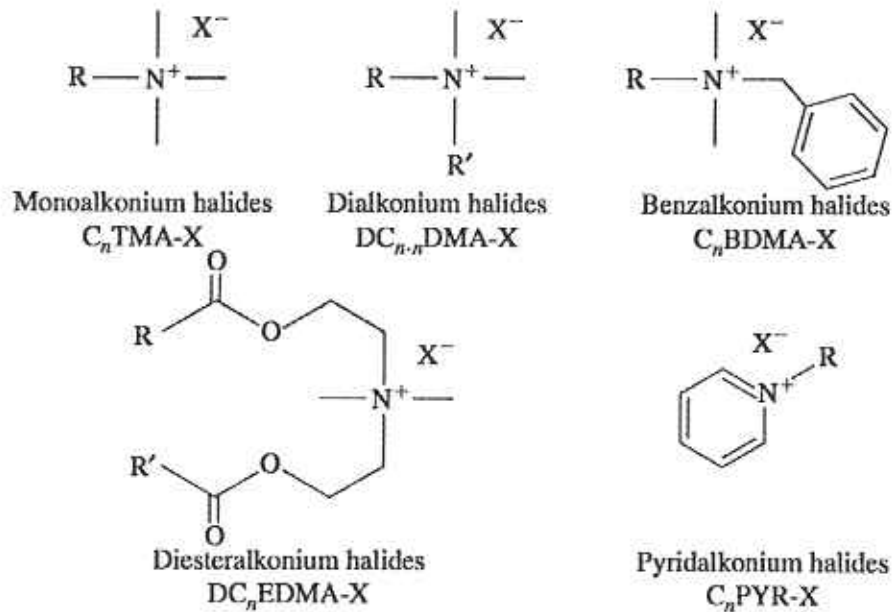


Figure 2.2. General structures of QAC subgroups (Tezel and Pavlostathis, 2011).

When exposed to QACs, microorganism first adsorbs the agent into its cell wall. Then, the cytoplasmic membrane is disrupted due to its reaction with the positively charged quaternary nitrogen. Following this, the intracellular material leaks from the cytoplasm and proteins, genetic material and the cell wall starts to be degraded by the cell's own enzymes. Thus, they interfere with the cellular integrity (McBain, et al., 2004; McDonnell and Russell, 1999). Gram-negative bacteria are intrinsically more resistant to QAC than Gram-positives because of their outer membrane which is an extra barrier for QACs. The resistance to QACs on the other hand may be developed through changes in the membrane or overexpression of efflux pumps (McDonnell and Russell 1999).

Benzalkonium chlorides (BACs) are a sub-group of QACs and have two methyl, one alkyl and one benzyl group attached to the central nitrogen atom (Figure 2.2). Their generic name is N-alkyl dimethyl benzyl ammonium chloride (Pryor and Brown, 1975). BACs are effective biocides which are active within a broad range of pH and effective on a broad spectrum of bacteria, fungi and viruses even at low concentrations. The application concentration of BACs is between of 400 to 500 mg/L in disinfectant products (Tezel and Pavlostathis, 2011). Due to their extensive usage in medical formulations ranging from eye drops to hand disinfectants (Hegstad, et al., 2010), their concentration in the domestic wastewater is between 20 to 300  $\mu\text{g/L}$  (Clara, et al., 2007). Hospital discharge on the other hand, contains BACs between 0.05 and 6.03 mg/L regardless of the size of the hospital (Kümmerer, et al., 1997; Tezel and Pavlostathis, 2011).

Throughout the years, biocide consumption at homes and hospitals has increased immensely. Unfortunately, it has been recently proven that resistance to antimicrobial agents such as triclosan and QACs and antibiotics share similar mechanisms. Therefore, this increase in the consumption of these disinfectants may contribute to evolution and rapid dissemination of resistance mechanisms which may then confer resistance to antibiotics (McDonnell and Russell, 1999; Akimitsu, et al., 1999)).

There are two important phenomena needed to be explained to better understand the relationship between antibiotic and QAC resistance: co-resistance and cross-resistance. The latter happens when a single mechanism works for more than one class of antimicrobial agent; a cross-resistant strain is one that has a single resistance mechanism which enables it to survive in the presence of different antimicrobial agents. The former term is used to explain the selection of a mobile genetic element which carry several genes of antimicrobial resistance (Wales and Davies, 2015). Thus, bacteria receiving this plasmid would have the genetic data to become resistant to multiple antimicrobial agents. The similarity of QAC resistance mechanisms to antibiotic resistance may lead to selection of co-resistant and cross-resistant strains at sub-inhibitory concentrations. Between these two, co-resistance to antibiotics is more likely to occur and some examples of co-resistance promoting efflux pumps are given in Table 2.1. Among these, plasmid encoded pumps are an easy way for bacteria to gain resistance when there is a selective pressure in the environment just as in wastewater treatment plants or in hospital discharge effluents.

Some of the acquired QAC resistance mechanisms are alterations in the membrane composition, overexpression of the chromosomal efflux pumps and acquisition of plasmid encoded efflux pumps (Hegstad, et al., 2010). Among these, resistance through efflux pumps is a genetically encoded transferable skill which also leads to antibiotic co-resistance through horizontal gene transfer. Resistance through efflux pumps occurs by overexpression of the pumps either by an intervention on the regulatory system to increase the efflux pumps or by mutation in the genetic element. Both mechanisms are triggered by the QAC concentration in the environment and further contribute to the antibiotic resistance in the environment due to co-resistance.

Biodegradation is another mechanism for bacteria to tolerate an antimicrobial agent. Beta-lactamases, which cleaves beta-lactam ring on beta-lactam antibiotics such as penicillin, are the best examples of enzymes that deactivates the biocides by biotransformation. Relatively recently, it was reported that some microorganism such as several species of the *Pseudomonas* biodegrade QACs (Tezel and Pavlostathis, 2011). The biodegradation of BACs commences by an attack of an

oxygenase enzyme called oxyBAC to the carbon of the alkyl chain adjacent to the nitrogen atom. This attack results in the cleavage of C-N bond and the formation of benzyl dimethyl amine and an alkanolic acid which are further utilized as carbon and energy source by the bacteria (Ertekin, 2017). The strains that degrade BACs are intrinsically resistant to that compound.

Biodegradation of BACs may decrease the efficacy of BAC containing disinfectants thus the performance of cleaning and disinfection in hospitals and homes creates hot-spots of poorly disinfected surfaces at low BAC concentrations. Bacteria which may be susceptible to BAC at their application dosages may survive on these hot-spots, acquire resistance genes from resistant bacteria and proliferate since aforementioned three prerequisites for resistance are attained due to biodegradation of BACs.

Given the fact that biodegradation of biocides is inevitable in hospitals, homes and environment, the main objective of this research is to elucidate and model the role of biodegradation on the development and dissemination of BAC resistance in a microbial community composed of a BAC degrader and a BAC susceptible microorganism.

Table 2.1. The specific efflux pumps and their effect on various antimicrobial agents (Hegstad, et al., 2010).

NAME	SPECIES	ANTIMICROBIAL AGENTS EXPORTED
<u>Plasmid-encoded efflux pumps</u>		
QacA	<i>Sta. aureus</i> and other staphylococci	BAC, Cetrimide, Chlorhexidine
OqxAB	<i>E. coli</i>	BAC, Triclosan, Chloramphenicol, Quinolones, Trimethoprim, Quinoxalines
<u>Chromosomally encoded efflux pumps</u>		
MdrL	<i>L. monocytogenes</i>	QACs, macrolides, cefotaxime
MdeA	<i>Sta. aureus</i>	BAC, fucidic acid, mupirocin, virginiamycin, novobiocin
MePA	<i>Sta. aureus</i>	BAC, chlorhexidine, pentamidine, fluoroquinolones
NorA	<i>Sta. aureus</i>	Cetrimide, BAC, fluoroquinolones
AcrAB-TolC	<i>E. coli</i>	QACs, triclosan, chlorhexidine, ampicillin, chloramphenicol, nalidixic acid, tetracycline, rifampicin
SdeXY	<i>Se. marcescens</i>	BAC, erythromycin, tetracycline, norfloxacin
mexCD-OprJ	<i>P. aeruginosa</i>	BAC, chlorhexidine, quinolones, macrolides, tetracyclines, lincomycin, chloramphenicol, novobiocin, meropenem, most penicillins, most cepheems
PmpM	<i>P. aeruginosa</i>	BAC, fluoroquinolones

### 3. APPROACH

The possibility of emergence and dissemination of BAC resistance was tested under varying BAC concentrations, driven by the biodegradation of the biocide in a simple microbial community composed of a resistant BAC degrader and a BAC susceptible microorganisms. *Pseudomonas sp.* BIOMIG1, isolated from sewage was used as the resistant BAC degrader in the experiments (Ertekin, 2017), whereas *Escherichia coli* was used as the BAC susceptible microorganism whose BAC MIC is 16 mg/L (Gül, 2013). Both are gram-negative, aerobic bacteria. Both microorganisms are known to co-exist in nature, in water treatment plants and in hospitals, with other microorganisms, under variable stress conditions. Tetradecyl benzyl dimethyl ammonium chloride (C<sub>14</sub>BDMA-Cl) was used as a substrate for BIOMIG1, while maltose was used for *E. coli*. Neither *E. coli* can degrade C<sub>14</sub>BDMA-Cl nor can BIOMIG1 utilize maltose. A co-culture system composed of the previously mentioned strains of bacteria was continuously fed with 16 mg/L, which is equal to the MIC for *E. coli*, and 1000 mg/L maltose. BAC degradation along with BIOMIG1 and *E. coli* growth were monitored throughout the operation. Resistant *E. coli*'s were identified using BAC agar plates on which no susceptible *E. coli* can grow.

A dynamic model which include bacterial growth, inhibition and mutation processes was developed, every parameter in model was estimated using experimental data obtained from batch experiments performed with individual microorganisms with and without BAC and finally verified using data obtained from continuous flow reactor system described above. Finally, the model was run to determine limiting BAC concentration for the resistant *E. coli* to proliferate.

## 4. MATERIALS & METHODS

### 4.1. Chemicals

The BACs mixture (BARQUAT 80) used in the experiments was obtained from Lonza Inc. (Basel, Switzerland) and contained a mixture of three benzalkonium chloride homologs: 40% (w/w) dodecyl benzyl dimethyl ammonium chloride ( $C_{12}$ BDMA-Cl, 340 g/mole,  $C_{21}H_{38}NCl$ ), 50% (w/w) tetradecyl benzyl dimethyl ammonium chloride ( $C_{14}$ BDMA-Cl, 368 g/mole,  $C_{23}H_{42}NCl$ ) and 10% (w/w) hexadecyl benzyl dimethyl ammonium chloride ( $C_{16}$ BDMA-Cl, 396.1 g/mole,  $C_{25}H_{46}NCl$ ) (Figure 4.1).

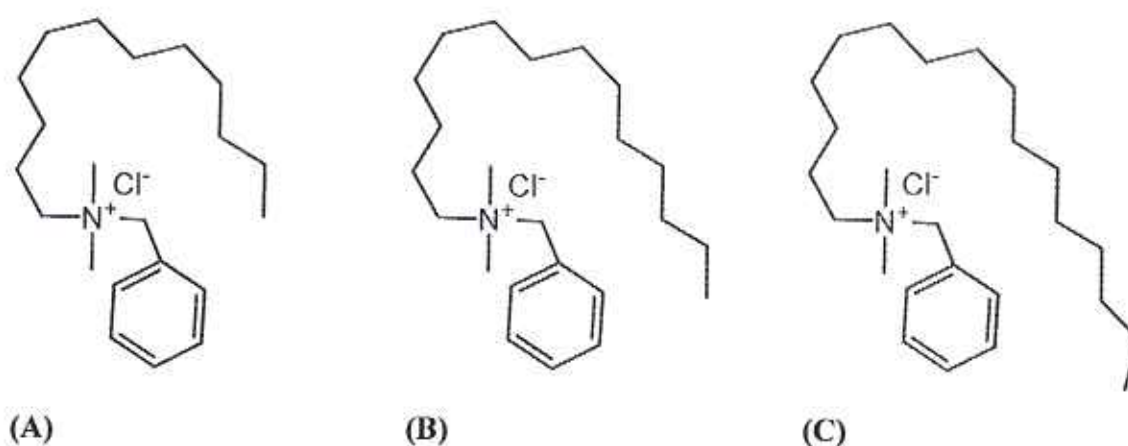


Figure 4.1. Chemical structure of (A)  $C_{12}$ BDMA-Cl, (B)  $C_{14}$ BDMA-Cl, (C)  $C_{16}$ BDMA-Cl.

High purity tetradecyl benzyl dimethyl ammonium chloride ( $C_{14}$ BDMA-Cl) used in the single BAC solutions was obtained from Tokyo Chemical Industry Co., Ltd., (Tokyo, Japan). High purity D (+) Maltose ( $C_{12}H_{22}O_{11}$ , 342.3 g/mole, Figure 4.2) used in the maltose solution was obtained from Merck and Sigma Aldrich Chemicals Company (Missouri, USA). All the organic solvents and mineral salts were obtained from Merck and Sigma Aldrich Chemicals Company.

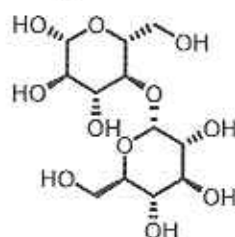


Figure 4.2. Chemical structure of maltose.

## 4.2. Microorganisms

### 4.2.1. Bacteria Strains Used in the Experiments

*Pseudomonas sp.* BIOMIG1<sup>BAC</sup> was used as the BAC-resistant, BAC degrading organism in the single culture and co-culture batch and continuous experiments (Ertekin, et al., 2016). Optimum growth temperature of BIOMIG1 is 28°C and it cannot grow at and above 35°C (Yilmaz, 2010). BIOMIG1 can degrade BACs but cannot utilize maltose as a carbon and energy source.

*Escherichia coli* was used as the BAC susceptible microorganism in the single culture and culture batch and continuous experiments. Optimum growth temperature for *E. coli* is 37°C, and it can also grow fast at temperatures between 20-30°C. *E. coli* can degrade maltose but cannot utilize BACs as a carbon and energy source (Gül, 2013).

### 4.2.2. Preparation of Cultures

A colony of *E. coli* grown on Luria Bertani (LB) agar was first incubated in 5 ml LB Broth (Table 4.2) overnight on an orbital shaker at 130 rpm at 37°C. Then, 1 mL of bacteria suspension was transferred into a microcentrifuge tube and centrifuged for 10 minutes at 10,000 rpm. The pellet was suspended with 1mL of %85 saline solution after discarding the supernatant. Same procedure was followed to grow BIOMIG1 but LB Broth (Table 4.2) containing 50 mg/L of BAC was used for the incubations at 25°C. Cell suspensions were used as inoculum in batch and continuous flow reactor experiments.

## 4.3. Characterization of *E. coli*

### 4.3.1. BAC Inhibition Assays

**4.3.1.1. In liquid medium.** MIC of BAC for *E. coli* was measured in 10-mL culture tubes. Twelve culture tubes with red-polypropylene caps were autoclaved. Three 100-mL aliquots of sterile salt medium (M9) containing only 1000 mg/L maltose (Solution-1) and 1000 mg/L maltose and 2048 mg/L BAC (Solution-2) and 1000 mg/L maltose which was inoculated with 0.5 mL *E. coli* suspension (Solution-3) were prepared (Table 4.1). A 1 mL Solution-3 was transferred to culture tubes containing 1 mL solution containing 1000 mg/L maltose and a range of BAC concentrations from 1 to 1024 mg/L were prepared by mixing Solution-1 and -2. The tubes were incubated at room

temperature (22 °C) for 24 hours and the growth measured with a UV/Vis spectrometer at 600 nm wavelength. Tubes containing M9 with only maltose having the same BAC concentrations but without any culture were used as blanks.

Table 4.1. The contents of the solutions.

Solution #	Content
Solution-1	1000 mg/L maltose
Solution-2	1000 mg/L maltose and 2048 mg/L BAC
Solution-3	1000 mg/L maltose and 0.5 mL of <i>E. coli</i> suspension

4.3.1.2. On Agar Plates. MIC of BAC for the *E. coli* on agar plates was determined by spreading three replicates of 100  $\mu$ L suspended *E. coli*, prepared as explained in section 4.2.2, on plates of different BAC concentrations. The plates were prepared as explained in section 4.6.1.2 with concentrations of 2, 4, 8, 16, 32, 64, 128, 256, 512 mg/L BAC. The growth on the plates were observed and the colony number was counted at each concentration for all three replicates.

#### 4.4. Batch Experiments

Batch experiments were performed to measure the BAC biodegradation, BIOMIG1 growth and *E. coli* growth rates when strains were inoculated individually and together, with and without BAC. One-liter media bottles with screw caps were used as reactors. Data were used to predict kinetic parameter used in the model developed. Experiments were set at four different conditions:

##### 4.4.1. *E. coli* in Maltose

Autoclaved 500 mL M9 medium (section 4.6.3) containing 1000 mg/L maltose was transferred into 1-L media bottle. A certain amount of active *E. coli* suspension was grown over night in 300 mg/L maltose it was then transferred into the bottle, aseptically, to set an initial turbidity of 0.01 at 600 nm. Once the inoculum was added, the reactor was agitated at 180 rpm for 3 days and the absorbance value was recorded throughout the experiment. Meanwhile, the samples were spread onto I.B plates once every three hours after diluting them with 0.85 % saline solution.

#### 4.4.2. *Pseudomonas sp.* BIOMIG1 in BAC

A colony of BIOMIG1 taken from an LB-BAC plate was grown in a glass tube containing 2 mL of M9 medium with 16 mg/L BAC on an orbital shaker set at 130 rpm. Once the biodegradation of BAC was completed, approximately in 3 days, 1 mL of solution was transferred into a 250-mL blue cap bottle containing 100 mL of M9 with 300 mg/L C<sub>14</sub>BDMA-Cl. The BAC amount in the medium was measured daily with HPLC and when the solution turned to a bright yellow and all the BACs in it was biodegraded, 9 mL of it was transferred into a 1L reactor bottle containing 500 mL of M9 with 16 mg/L of C<sub>14</sub>BDMA-Cl. This reactor was then set on a stirrer at 180 rpm and BAC biodegradation was measured hourly with HPLC. At the same time, after appropriately diluting it with 0.85 % saline solution, three replicates from it were spread onto LB-HiBAC plates once every 3 hours until the degradation was complete.

#### 4.4.3. *E. coli* in Maltose and BAC

The same procedure in section 4.4.1 was followed but the medium contained 16 mg/L C<sub>14</sub>BDMA-Cl instead of 1000 mg/L maltose. The samples were spread onto both LB and LB-HiBAC plates followed by appropriate dilution with 0.85 % saline solution.

#### 4.4.4. *E. coli* and *Pseudomonas sp.* BIOMIG1 in Maltose and BAC

Prior to setting up the reactor, *E. coli* was grown in M9 with 300 mg/L maltose and *P. sp.* BIOMIG1 was grown in M9 with 300 mg/L BAC as explained in sections 4.4.1 and 4.4.2. 500 mL of M9 media in a 1L bottle containing 5 mL of 100 g/L maltose stock solution was used as the reactor. When the bacteria were grown in their separate medium, first *E. coli* was spiked into the medium until an absorbance value of 0.010 was reached at 600 nm wavelength. This was followed by the addition of 9 mL of *P. sp.* BIOMIG1. As a last step, 0.625 mL of 12.8g/L C<sub>14</sub>BDMA-Cl stock solution was added into the reactor to reach a concentration of 16 mg/L of BAC.

The reactor was set on a stirrer and stirred at 180 rpm for 5 days. Biodegradation of BAC was measured with HPLC, the absorbance at 600 nm was recorded all along and the samples were spread onto LB and 256 mg/L LB-HiBAC plates after diluting with 0.85 % saline solution. The LB plates were placed in the incubator at 37°C overnight, while LB-BAC plates were set at room temperature for 2 days. In addition to this, a separate spread was executed onto LB-HiBAC plates without dilution and placed in the incubator at 37°C along with LB plates as control.

## 4.5. Continuous Flow Experiments

A continuous-flow reactor system was set to determine the dynamics of *E. coli* and BIOMIG1 interactions with each other and growth substrates under continuous physical and chemical stress conditions such as BAC and dilution. The data obtained in this set of experiments are used to verify the model and to determine conditions to prevent resistance evolution and dissemination.

### 4.5.1. *E. coli* in Maltose

The reactor contained 500 mL of M9 medium with 1000 mg/L maltose and *E. coli* inoculum prepared as in the batch system (4.4.1) in a 2-L media bottle with a screw cap. The reactor was fed with sterile M9 medium containing 1000 mg/L maltose from the inlet port and same volume of mixed liquor was withdrawn from the reactor using a BIO-RAD EP-1 Econo multi-channel peristaltic pump (BIO-RAD laboratories, CA, USA) as in Figure 4.3. After setting the silicone tubing aseptically, the reactor was settled on a stirrer at 180 rpm, and the pumps was set at 0.88 mL/min ( $D = 0.1 \text{ hr}^{-1}$ ).

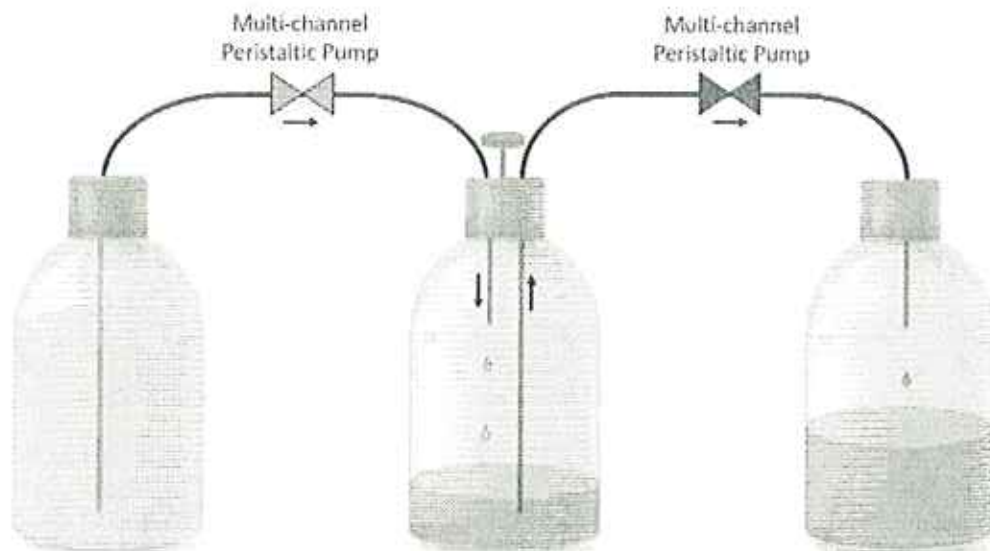


Figure 4.3. An illustration of the continuous-flow reactor system.



Figure 4.4. Picture of the continuous-flow reactor system.

The samples were taken from the outlet of the reactor aseptically twice a day. The absorbance at 600 nm wavelength was recorded with a UV-Vis Spectrometer. Three replicates of each sample were spread onto LB plates after they were appropriately diluted with 0.85 % saline solution. As control, 100  $\mu$ L of 3 replicate of each sample were spread onto 256 mg/L LB-BAC plates. The colony number of each plate was recorded after 24 hours of incubation at 37°C.

#### 4.5.2. *P. sp.* BIOMIG1 in BAC

The procedure followed to set up the continuous reactor system for *P. sp.* BIOMIG1 was the same as in Section 4.5.1. A 2L glass bottle containing 500 mL of M9 medium with 16 mg/L BAC was used as the reactor. This reactor was fed with M9 medium with 16 mg/L BAC at 0.88 mL/min flow rate and the effluent was transferred into another sterile bottle. Three replicates of each sample were spread onto 256 mg/L LB-BAC plates after appropriately diluted with 0.85 % saline solution. The colony number of each plate was recorded after 24 hours of incubation at 25°C. In addition, BAC concentration in the samples was measured using the HPLC method described below.

### 4.5.3. *E. coli* and *P. sp.* BIOMIG1 in Maltose and BAC

A similar procedure described for only *E. coli* and BIOMIG1 continuous flow reactor systems was followed to set up a reactor system with both *E. coli* and BIOMIG1. The reactor was initiated with co-culture of *E. coli* and BIOMIG1 in M9 medium containing 1000 mg/L maltose and 16 mg/L BAC and fed with the same medium at flowrate of 0.88 mL/min. This was followed by 1000 mg/L of maltose and 16 mg/L BAC addition. Samples were collected aseptically from the outlet twice a day for over 10 days. Three replicate of each sample were spread onto both LB and 256 mg/L LB-BAC plates. The LB plates were incubated at 37°C to eliminate *P. sp.* BIOMIG1 growth and the LB-BAC plates were incubated at 25°C. As control, the samples were spread onto 256mg/L LB-BAC plates and incubated at 37°C without any dilution to monitor BAC resistance of *E. coli*.

## 4.6. Media, Broth and Agar Plates

### 4.6.1. Luria Bertani (LB) Broth

LB Broth was prepared by autoclaving a solution of 1L DI water containing 10 g tryptone, 5 g yeast extract and 5 g NaCl for 15 minutes at 121°C (Table 4.2).

Table 4.2. Chemical composition of LB Broth.

Chemical	Concentration (g/L)
NaCl	5.00
Tryptone	10.00
Yeast Extract	5.00

### 4.6.2. LB-BAC Broth

LB-BAC Broth was prepared and autoclaved the same way as LB Broth (Table 4.2). Following the sterilization, 5mL of 10g/L BACs stock solution was added to the mixture to obtain a final BAC concentration of 50 mg/L once the solution was cooled.

### 4.6.3. Mineral Salt Medium (M9)

M9 medium is prepared by adding the  $K_2HPO_4$ ,  $KH_2PO_4$ , NaCl,  $NH_4Cl$  and the trace metal solution at specified amounts in to a 1L DI water. The content is autoclaved for 15 minutes at  $121^\circ C$  followed by addition of  $MgSO_4 \cdot 7H_2O$  and  $CaCl_2$  after the solution is cooled in order to prevent scaling (Table 4.3 and Table 4.4).

Table 4.3. Composition of M9 medium.

Chemical	Concentration (g/L)
$K_2HPO_4$	7.40
$KH_2PO_4$	3.00
NaCl	0.50
$NH_4Cl$	1.00
Trace metal stock solution	1.00
$MgSO_4 \cdot 7H_2O$	0.25
$CaCl_2$	0.01

Table 4.4. Composition of the trace metal stock solution.

Chemical	Concentration (g/L)
$CoCl_2 \cdot 6H_2O$	2.00
$CuCl_2 \cdot 2H_2O$	0.10
$H_3BO_3$	3.00
$MnCl_2 \cdot 4H_2O$	0.30
$Na_2MoO_4 \cdot 2H_2O$	0.30
$NiSO_4 \cdot 6H_2O$	0.20
$ZnCl_2$	0.50

### 4.6.1. Plates

4.6.1.1. LB Agar Plates. LB agar plates were prepared by autoclaving a solution of 1L DI water with 10 g tryptone, 5g yeast extract, 5g NaCl and 15 g agar for 15 minutes at  $121^\circ C$ . The solution was poured to petri dishes aseptically after being cooled to  $50^\circ C$ .

4.6.1.2. LB-BAC Plates. LB-BAC plates were prepared and autoclaved the same way as LB agar plates. When they were cool enough to be poured, the necessary BAC amount was added from the BACs stock solution to obtain a final BAC concentration of 50 mg/L.

4.6.1.3. LB-HiBAC Plates. LB-HiBAC plates were prepared the same way as LB-BAC plates but at 256 mg/L BAC concentration.

4.6.1.4. CHROM<sup>TM</sup> Agar ECC Agar Plates. Chromagar ECC plates were prepared by adding 32.8 g of ECC agar (CHROMagar Microbiology, France) into 1L of DI water. This was then poured into plates aseptically after being heated and stirred on a hot plate until it reaches its boiling point.

4.6.1.5. CHROM<sup>®</sup> Agar Pseudomonas<sup>TM</sup> Plates. Chromagar Pseudomonas plates were prepared by adding 33.2 g of PS agar (CHROMagar Microbiology, France) into 1L of DI water. This was then poured into plates aseptically after being heated and stirred on a hot plate until it reaches its boiling point.

#### **4.6.2. 0.85 % Saline Solution**

A sodium chloride solution of 0.85 % was prepared in a volumetric flask and transferred to a blue cap bottle and autoclaved at 121°C for 15 minutes. The bottles containing the saline solution was autoclaved after each usage throughout the experiments.

#### **4.6.3. BACs Stock Solution**

A stock solution of 10 g/L BACs was prepared by dissolving 0.125 g BARQUAT 80 (a mixture of BAC mixture of 32% C<sub>12</sub>BDMA-Cl, 40% C<sub>14</sub>BDMA-Cl, 8% C<sub>16</sub>BDMA-Cl and 20% ethanol) in 10 ml DI water.

#### **4.6.4. C<sub>14</sub>BDMA-Cl Stock Solution**

A stock solution of 12.8 mg/L of C<sub>14</sub>BDMA-Cl was prepared by dissolving 0.28 g of C<sub>14</sub>BDMA-Cl in 100 mL DI water.

#### 4.6.5. Maltose Stock Solution

Stock solution of 100 g/L maltose was prepared by adding 10.5 g of maltose in to 100 mL of DI water and autoclaving at 121°C for 15 minutes.

### 4.7. Analytical Methods

#### 4.7.1. BAC Analysis

Throughout the experiments BAC analysis was done as Ertekin et al (Ertekin, 2016). Concentration of BACs in the samples were measured with an Agilent1260 Series HPLC (Agilent Technologies, CA, USA) using a Phenomenex Luna SCX column (250 x 4.6 mm, 5 $\mu$ ) (Phenomenex, Inc., CA, USA) followed by a Polaris C<sub>18</sub>A column (50 X 4.6 mm, 3.2 $\mu$ ) (Agilent Technologies, CA, USA). Additionally, a Phenomenex SCX SecurityGuard cartridge (4 x 3.0 mm) was used as a guard column.

The eluent was composed of a 60:40 (v/v) combination of acetonitrile and 50 mM phosphate buffer (pH 2.5) and was given to the columns at a flow rate of 1.0 mL/min. The column temperature was set at 35°C. UV-Vis diode array detector was used for the detection of QACs at 210 nm. The samples were mixed in 1:1 with the eluent beforehand. They were centrifuged and 0.7 mL of the supernatant was transferred into the HPLC vials for the analysis.

HPLC chromatogram of BACs and the calibration curves are given in Figure 4.5 and Figure 4.6 respectively.

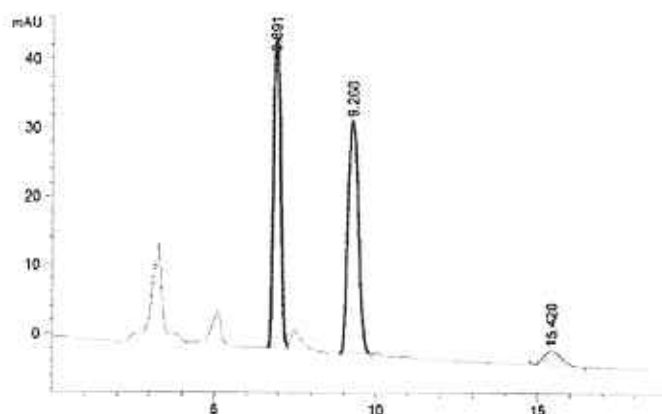


Figure 4.5. Representative HPLC chromatogram of C<sub>12</sub>BDMA-Cl in red, C<sub>14</sub>BDMA-Cl in blue and C<sub>16</sub>BDMA-Cl in green.

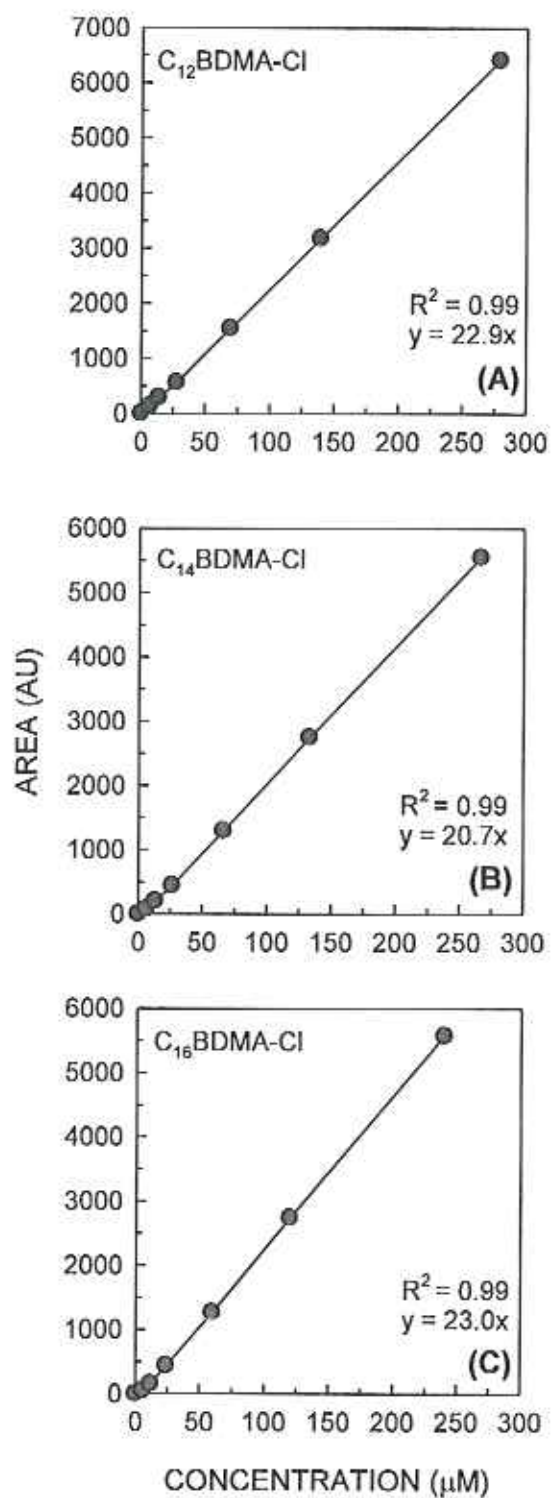


Figure 4.6. Calibration curves of  $\text{C}_{12}\text{BDMA-Cl}$ ,  $\text{C}_{14}\text{BDMA-Cl}$  and  $\text{C}_{16}\text{BDMA-Cl}$ .

## 5. MODEL STRUCTURE AND EQUATIONS

### 5.1. System Description

The biological system that was modeled in this study composed of two microorganisms and two substrates. *Pseudomonas* sp. BIOMIG1 utilizes C<sub>14</sub>BDMA-Cl as the sole carbon and energy source whereas *E. coli* consumes maltose. BIOMIG1 cannot use maltose and *E. coli* does not consume C<sub>14</sub>BDMA-Cl. C<sub>14</sub>BDMA-Cl also serves as an inhibitor in the system since it is a biocide. BIOMIG1 can tolerate C<sub>14</sub>BDMA-Cl up to 1024 mg/L (2.8 mM) whereas *E. coli* is inhibited by C<sub>14</sub>BDMA-Cl at and above 16 mg/L (43 μM). This system can be operated both in batch and continuous modes. In the batch mode substrates are the limiting factors. But the dilution rate is the biomass controlling factor when the system is operated in the continuous mode.

### 5.2. Model Processes

There are four main processes in the model system: (1) Substrate degradation, (2) Biomass growth and decay, (3) Inhibition of maltose utilization by *E. coli*, and (4) Transformation of susceptible *E. coli* to BAC resistant *E. coli* via random mutations or gene transfer (Figure 5.1).

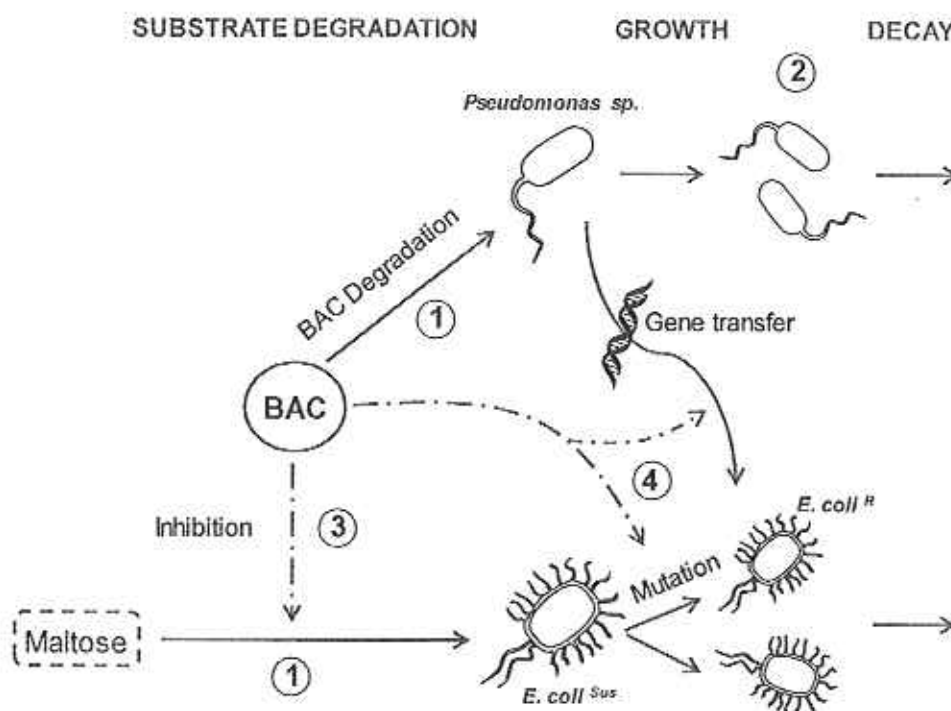


Figure 5.1. Biological processes in the model system.

Process-1 includes BAC and maltose biodegradation by BIOMIG1 and *E. coli*, respectively. Process-2 involves growth of BIOMIG1 and *E. coli* on BAC and maltose as the sole carbon sources, respectively. BAC inhibits maltose utilization by *E. coli* and amplifies the decay (Process-3). Therefore, Process-3 interacts with Process-1 and -2. Process-4 is the transformation of susceptible *E. coli* to resistant *E. coli* via mutation and gene transfer. Resistant *E. coli* generated by Process-4 also degrades maltose and grows. Therefore, Process-4 interacts with both Process-1 and -2 (Figure 5.1).

### 5.3. Model Equations

Variables and constants used in the model are given in Table 5.1. Utilization of BAC (Equation 5.1) and maltose (Equation 5.2) by BIOMIG1 and *E. coli*, respectively (Process-1) and their growth on those substrates (Process-2; Equation 5.4 and 5.5) were modeled using Monod growth kinetics. Flow of substrates and microorganisms in and out of the system were also included in the model using dilution rate ( $D, T^{-1}$ ) which is the ratio of the flow rate ( $Q$ ) to the liquid volume ( $V$ ) in the reactor.

Table 5.1. Definitions of the parameters used in the model equations.

Parameter	Definition	Unit
$S_i$	Substrate, $i$ is either BAC or Maltose	$\mu\text{M}$
$Q$	Flow rate	$\text{mL/hr}$
$V$	Volume	$\text{mL}$
$X_m$	Microorganism concentration, $m$ is Ec or Ps which stands for <i>E. coli</i> or <i>Pseudomonas sp.</i> BIOMIG1. Superscript S refers to susceptible, R refers to resistant	$\text{cell/L}$
$Y_i$	Cell yield on substrate $i$	$\text{cell}/\mu\text{mole } S_i$
$k_i$	Maximum utilization rate constant for substrate $i$	$\mu\text{mole/hr-cell}$
$k_d$	Decay rate constant for cells	$\text{hr}^{-1}$
MIC	Minimum inhibitory concentration	$\mu\text{M}$
$K_i$	Half saturation coefficient for the substrate $i$	$\mu\text{M}$

Inhibition of maltose utilization of *E. coli* is introduced into the Equation 5.2 by the *Inh* function as a multiplier. The *Inh* function is equal to 0 when the BAC concentration is equal to or above the MIC for susceptible *E. coli*. It approaches 1 as BAC concentration reaches 0. This

function is active only when BAC is present in the medium. The magnitude of the inhibition is variable and decreases as the BAC concentration decreases. One other role of the *Inh* function is to introduce the competition between susceptible and resistance *E. coli* in the model. As the BAC won't inhibit the maltose degradation of resistant *E. coli*, resistant *E. coli* will be selected over the susceptible *E. coli* when BAC is present in the medium which is implied in **Equation 5.2** with the absence of the *Inh* function as a multiplier for the maltose degradation of the resistant *E. coli*.

$$\frac{\partial(S_{BAC})}{\partial t} = \frac{Q}{V} \cdot S_{BAC}^0 - \frac{Q}{V} \cdot S_{BAC} \cdot \frac{k_{BAC} \cdot S_{BAC} \cdot X_{Ps}}{K_{BAC} + S_{BAC}} \quad (5.1)$$

$$\frac{\partial(S_{Malt})}{\partial t} = \frac{Q}{V} \cdot S_{Malt}^0 - \frac{Q}{V} \cdot S_{Malt} \cdot \frac{k_{Malt} \cdot S_{Malt} \cdot X_{Ec}^S}{K_{Malt} + S_{Malt}} \cdot \mathbf{Inh} - \frac{k_{Malt} \cdot S_{Malt} \cdot X_{Ec}^R}{K_{Malt} + S_{Malt}} \quad (5.2)$$

$$\mathbf{Inh} = \text{IF } S_{BAC} \geq \text{MIC THEN } 0 \text{ ELSE } (1 - \frac{S_{BAC}}{\text{MIC}}) \quad (5.3)$$

Growth consists of cell production coupling with substrate utilization and cell decay (Process-2; **Equation 5.4, 5.5 and 5.6**). When BAC is present, the production rate of susceptible *E. coli* decreases since maltose degradation is inhibited (Process-3). Additionally, the decay rate of susceptible *E. coli* cells increases due to the disinfection effect of BACs. The effect of BAC on the decay rate is included in **Equation 5.5** as an exponential effect, referred with the *Rec* function. One more sink for the susceptible *E. coli* is their transformation to resistant cells in the presence of BAC (Process-4). This transformation process is included in **Equation 5.5** with the *Trans* function. The transformation process is the main source for resistant *E. coli* cells which then grow and decay. It should be noted that resistant *E. coli* cells do not get inhibited by BAC.

$$\frac{\partial(X_{Ps})}{\partial t} = \frac{Q}{V} \cdot X_{Ps}^0 - \frac{Q}{V} \cdot X_{Ps} + Y_{BAC} \cdot \frac{k_{BAC} \cdot S_{BAC} \cdot X_{Ps}}{K_{BAC} + S_{BAC}} - k_d \cdot X_{Ps} \quad (5.4)$$

$$\frac{\partial(X_{Ec}^S)}{\partial t} = \frac{Q}{V} \cdot X_{Ec}^{S0} - \frac{Q}{V} \cdot X_{Ec}^S + (1 - \mathbf{Trans}) \cdot Y_{Malt} \cdot \frac{k_{Malt} \cdot S_{Malt} \cdot X_{Ec}^S}{K_{Malt} + S_{Malt}} \cdot \mathbf{Inh} - k_d \cdot (X_{Ec}^S)^{\mathbf{Rec}} \quad (5.5)$$

$$\frac{\partial(X_{Ec}^R)}{\partial t} = \frac{Q}{V} \cdot X_{Ec}^{R0} - \frac{Q}{V} \cdot X_{Ec}^R + Y_{Malt} \cdot \frac{k_{Malt} \cdot S_{Malt} \cdot X_{Ec}^R}{K_{Malt} + S_{Malt}} - k_d \cdot X_{Ec}^R + \mathbf{Trans} \cdot Y_{Malt} \cdot \frac{k_{Malt} \cdot S_{Malt} \cdot X_{Ec}^S}{K_{Malt} + S_{Malt}} \cdot \mathbf{Inh} \quad (5.6)$$

Alongside the *Inh* function which is used to regulate maltose degradation by susceptible *E. coli* cells due to inhibition, the *Rec* and *Dead* functions are used to enhance decay when BAC is present (**Equation 5.7 and 5.8**). The *Trans* function is used as a valve to regulate the formation of resistant

*E. coli* from susceptible ones (Equation 5.9). The *Rec* is active when BAC concentration is above the *UP* value which is the highest BAC concentration that promotes transformation of resistant *E. coli* cells. *Rec* is equal to the ratio of the BAC concentration and the MIC, and always greater than 1. The *Dead* function is active at BAC concentrations between *MIC* and *UP*. This concentration window promotes enhanced decay with a value equal to *Enh* although concentration is below the MIC. The *Trans* function is active at BAC concentrations between *UP* and *LOW*. This concentration range is defined as “transformation window” or “mutation window” which is the range of BAC concentration where transformation of susceptible cells to resistant ones at a random probability value of *P* which is between 0 and  $10^{-6}$  (Ibargüen-Mondragón, et al., 2014; Gullberg, et al., 2011)

$$\mathbf{Rec} = \text{IF } S_{\text{BAC}} \leq \text{MIC} \text{ THEN } \mathbf{Dead} \text{ ELSE } \frac{S_{\text{BAC}}}{\text{MIC}} \quad (5.7)$$

$$\mathbf{Dead} = \text{IF } S_{\text{BAC}} \leq \text{UP} \text{ THEN } 1 \text{ ELSE } \mathbf{Enh} \quad (5.8)$$

$$\mathbf{Trans} = \text{IF } S_{\text{BAC}} \leq \text{UP} \text{ AND } S_{\text{BAC}} \geq \text{LOW} \text{ THEN } \text{RANDOM}(0, P) \text{ ELSE } 0 \quad (5.9)$$

#### 5.4. Baseline Values and Data Interpretations

There are several unknown parameters in the equations. To find a reasonable range for those parameters, literature values were used (Table 5.2). These values were then converted to their unit equivalent using empirical conversion factors which were derived experimentally (Table 5.3).

The baseline values of the growth parameters used in the model were calculated as well. These values were then used for initial simulation of the model for mono-culture batch experiments, for instance *E. coli* in maltose and BIOMIG1 in BAC, and also to set a value range for prediction of unknown parameters.

Table 5.2. Literature values for BOD based substrate utilization and growth kinetics constants (Rittmann, et al., 2001).

Parameter	Carbohydrate BOD	Other BOD
	Value	Value
$f_s$	0.7	0.6
$Y, \text{gVSS/gBOD}_L$	0.49	0.42
$k, \text{gBOD}_L / \text{gVSS-d}$	27	20
$\mu^{\max}$ ,	13.2	8.4
$k_d$	0.05 – 0.3	0.05 – 0.3

Table 5.3. Conversion factors used to synchronize units of literature values with model units.

Parameter	Value
1 cell	$2.8 \times 10^{-13} \text{ g}$ $2.24 \times 10^{-13} \text{ gVS}$ $3.18 \times 10^{-13} \text{ gCOD}$
1 mole $C_{14}BDMA (C_{23}H_{42}N^+)$	332.5 g 130 ccq 1040 gCOD
1 mole Maltose ( $C_{12}H_{22}O_{11}$ )	342.3 g 48 ccq 384 gCOD

Table 5.4. Baseline values of growth parameters calculated based on literature values (Rittmann and McCarty, 2001).

Parameter	Value
<u><i>C<sub>14</sub>BDMA degradation by P.sp BIOMIG1</i></u>	
$k_{BAC}, \mu\text{mol BAC/cell-hr}$	$1.8 \times 10^{-10}$
$Y_{BAC}, \text{cells}/\mu\text{mol BAC}$	$1.95 \times 10^9$
$k_d, \text{hr}^{-1}$	0.0021 – 0.0125
<u><i>Maltose degradation by E. coli</i></u>	
$k_{\text{malt}}, \mu\text{mol maltose/cell-hr}$	$6.6 \times 10^{-10}$
$Y_{\text{Malt}}, \text{cells}/\mu\text{mol maltose}$	$8.40 \times 10^8$
$k_d, \text{hr}^{-1}$	0.0021 – 0.0125

Other values were either given as constants or their values were determined experimentally or through prediction.

Table 5.5. Other parameters, constants and initial values.

Parameter	Value	Method
Initial BAC ( $\mu\text{M}$ )	Measured	Analytical
Initial Maltose ( $\mu\text{M}$ )	Measured	Analytical
Initial $X_{PS}$ (cell/L)	Measured	Plate count, O.D.
Initial $X_{Ec}$ (cell/L)	Measured	Plate count, O.D.
$D$ ( $\text{hr}^{-1}$ )	Set	Pump setting
$M_{BAC}$ ( $\mu\text{M}$ )	1	Fixed, Experimental
$M_{\text{malt}}$ ( $\mu\text{M}$ )	1.13	Fixed, Experimental
MIC ( $\mu\text{M}$ )	43	Fixed, Experimental
UP ( $\mu\text{M}$ )	Predicted	Curve fitting to data
LOW ( $\mu\text{M}$ )	Predicted	Curve fitting to data
P	Predicted	Curve fitting to data
Enh	Predicted	Curve fitting to data

The Simulations and curve fitting were performed by using Berkeley Madonna v.8.0 software with Runge-Kutta integration method and root-mean-square deviation (RMSD) minimization.

### 5.5. Estimating the Parameter Values from the Experimental Data

The successive processes followed during the research can be seen from Figure 5.2 where the experimental part is followed by the model development. The experiment set used to estimate a specific parameter is given in Table 5.6. The MIC value was determined from the BAC susceptibility test of *E. coli* and set at 43  $\mu\text{M}$  to begin with. Then, the cell yield ( $Y_{PS}$ ) and the maximum utilization rate constant ( $k_{BAC}$ ) of BAC was estimated using the batch BIOMIG1 growth experiment. Specifically, to predict these, the BAC concentration data, given in Figure 6.2A, was fitted to the BAC concentration estimation of the model. The range within which the parameters were estimated was calculated from the baseline values extracted from the literature. The baseline value for  $k_{BAC}$  was set at  $1.8 \times 10^{-10}$   $\mu\text{mol BAC}/\text{cell}\cdot\text{hr}$  and the baseline value for  $Y_{PS}$  was set at  $1.95 \times 10^9$  cells/ $\mu\text{mol BAC}$  as in Table 5.4.

Similarly, the cell yield ( $Y_{Ec}$ ) and the maximum utilization rate constant ( $k_{\text{Malt}}$ ) of Maltose was estimated using the batch *E. coli* growth experiment. This was done by fitting the *E. coli* growth data in Figure 6.3B, obtained from the absorbance values, to the *E. coli* growth, estimated by the

model. Again, the range within which the estimation was done was determined from the baseline values given in Table 5.4. According to this, the baseline for  $k_{Malt}$  was set at  $6.6 \times 10^{10}$   $\mu\text{mol}$  maltose/cell-hr and the baseline for  $Y_{Malt}$  was set at  $8.40 \times 10^8$  cells/ $\mu\text{mol}$  maltose.

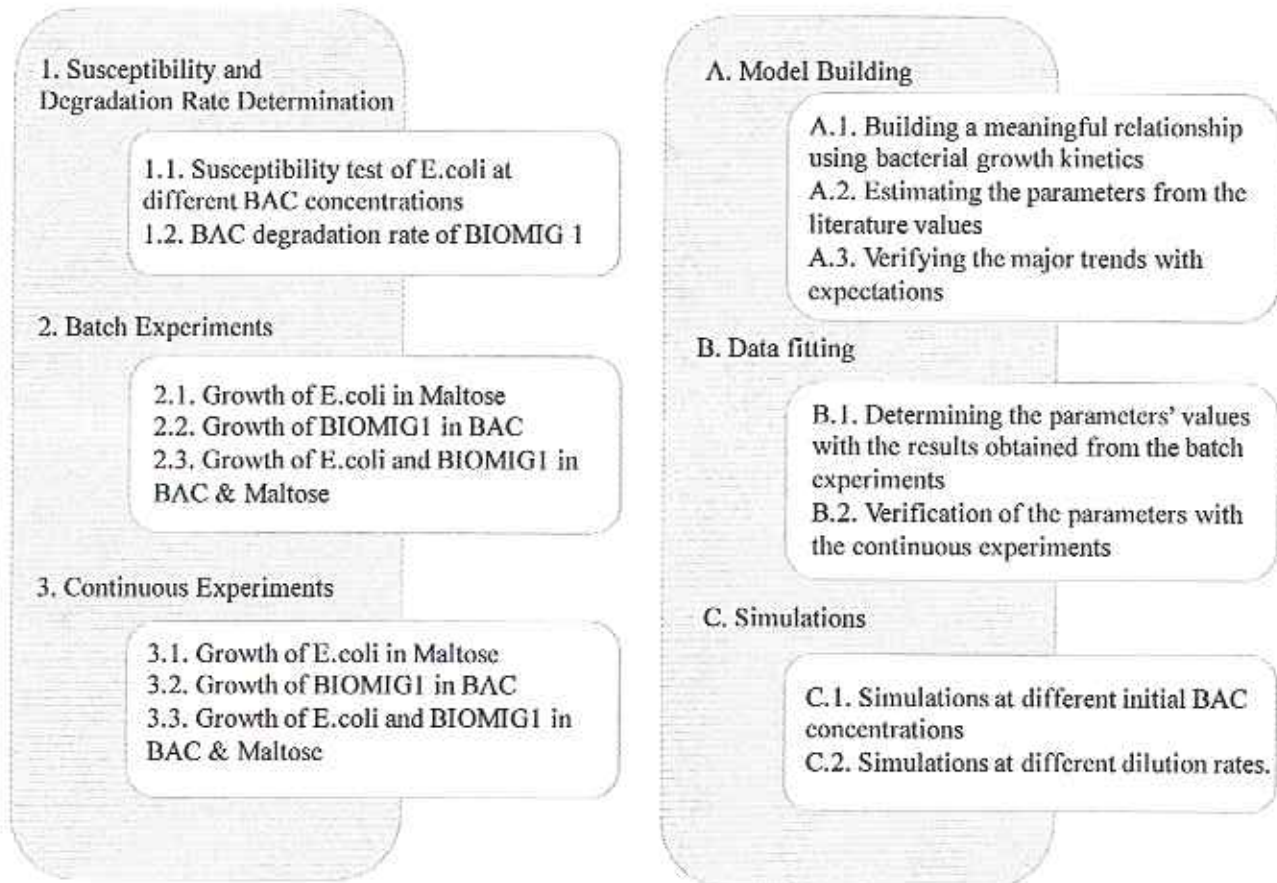


Figure 5.2. The experimental and the modelling processes.

Table 5.6. The experiment used for each fitted parameter.

Experiment	Parameter
Growth of BIOMIG1 in batch reactor (2.2)	$k_{BAC}$ ( $\mu\text{mol/hr} \cdot \text{cell}$ )
Growth of <i>E. coli</i> in batch reactor (2.1)	$k_{Malt}$ ( $\mu\text{mol/hr} \cdot \text{cell}$ )
Growth of <i>E. coli</i> in batch reactor (2.1)	$Y_{Ec}$ ( $\text{cell}/\mu\text{M } S_{Malt}$ )
Growth of BIOMIG1 in batch reactor (2.2)	$Y_{Ps}$ ( $\text{cell}/\mu\text{M } S_{BAC}$ )
Both (2.1) and (2.2)	$k_d$ ( $\text{hour}^{-1}$ )
Susceptibility test of <i>E. coli</i> (1.1)	MIC ( $\mu\text{M}$ )
Co-culture batch experiment (2.3)	UP ( $\mu\text{M}$ )
Co-culture batch experiment (2.3)	Enh ( $\mu\text{M}$ )
Co-culture continuous experiment (3.3)	LOW ( $\mu\text{M}$ )
Co-culture continuous experiment (3.3)	P

The decay rate constant ( $k_d$ ) was estimated again by fitting the *E. coli* growth data and BAC degradation data in Figure 6.2A and Figure 6.3B. The baseline range was calculated again as explained in section 5.4 and set between  $0.0021 \text{ hr}^{-1}$  and  $0.125 \text{ hr}^{-1}$ .

Furthermore, the *UP* and *Enh* values were estimated by fitting the *E. coli* growth data of the co-culture batch experiment as shown in Figure 6.7B. The estimation range of the *UP* value was set between  $0 \text{ }\mu\text{M}$  and  $43 \text{ }\mu\text{M}$ , which was the range of the possible BAC concentrations below the MIC level. The estimation range of *Enh* was set between 1 and 2, as it should be higher than 1 so that it increases the decay, but lower than 2 as the model gives illogical results when the effect is too high on the decay rate. Finally, the *LOW* and *P* values were estimated by fitting the resistant *E. coli* growth data of the co-culture continuous experiment. The range of *LOW* was set between  $0 \text{ }\mu\text{M}$  and  $22 \mu\text{M}$  which equals the previously estimated *UP* value. The baseline of *P* was set at  $1 \times 10^{-6}$  which was the literature value of the probability of occurrence of mutations.

The estimation of the parameters was mostly done with the curve-fitter feature of the Berkeley Madonna v.8.0, with root-mean-square deviation (RMSD) minimization. Two parameters were estimated at each fitting run at most and  $R^2$  values between the experimental datasets and their equivalent model estimations were calculated using the "RSQ" function of Microsoft Excel v.15.28.

## 6. RESULTS & DISCUSSION

### 6.1. Characterization of *E. coli*

Before starting the experiments, *E. coli* was characterized and the inhibitory BAC concentration was determined in liquid mineral salt medium and in agar plates following the procedures described in section 4.3.1. Turbidity in each test tube containing 1000 mg/L of maltose and 0, 2, 4, 8, 16, 32, 64, 128, 256, 512, 1024 mg/L BAC was measured at 600 nm wavelength. An absorbance value higher than 0.01AU was considered as growth. After 24 hours of incubation at 37°C, *E. coli* grew only at 2 and 4 mg/L BAC concentrations. Growth was almost totally inhibited at and above 8 mg/L BAC suggesting that MIC of BAC for *E. coli* is 16 mg/L or 43  $\mu$ M (Figure 6.1)

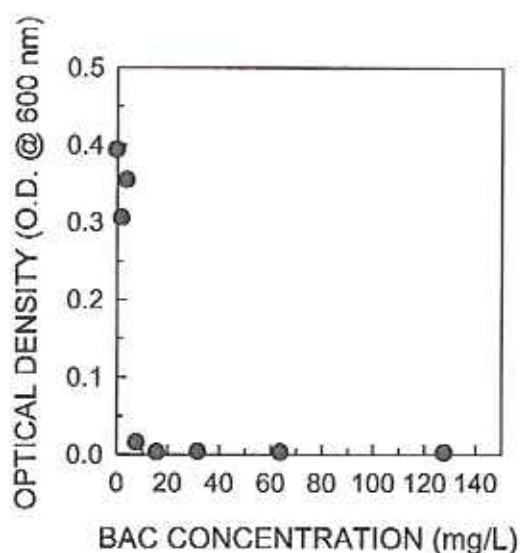


Figure 6.1. Optical density in tubes containing maltose and inoculated with *E. coli* between 2 and 1024 mg/L BAC concentration.

The inhibition concentration of BAC in solid agar plates was determined as well. Following incubation of the plates at 37°C colonies were observed on plates prepared at 2, 4, 8, 16, 32, 64, 128 mg/L of BAC while there was no growth on plates having 256 and 512 mg/L BAC.

From these results, the inhibition concentration of BAC was determined to be 16 mg/L and 256 mg/L in liquid and in solid medium respectively. These concentrations were used throughout the experiments as inhibitory concentrations.

## 6.2. Model Calibration

### 6.2.1. BAC Degradation in Batch Reactors by *Pseudomonas* sp. BIOMIG1

The batch experiment, testing the biodegradation of C<sub>14</sub>BDMA-Cl ( $S_{BAC}$ ) by *Pseudomonas* sp, BIOMIG1 ( $X_{Ps}$ ) lasted almost 30 hours. Initial concentration of BAC and BIOMIG1 was 41.6  $\mu$ M and  $1 \times 10^8$  cells/L. BAC was completely utilized in 12 hours (Figure 6.2A) and BIOMIG1 concentration reached to  $1 \times 10^{10}$  cells/L in the reactor (Figure 6.2B). The model simulated the BAC degradation with a good precision ( $R^2 = 0.95$ ) however failed to estimate the BIOMIG1 density correctly ( $R^2 = 0.60$ ) when baseline parameter values were used and  $k_d$  was set to 0.0021 hr (Table 5.4).

To improve the goodness of fit, the model was fit with experimental data and  $k_{BAC}$  and  $Y_{BAC}$  were predicted while other parameters related to BIOMIG1 growth were fixed. Precision of the simulation of BAC biodegradation increased to 0.99 (Figure 6.2A) while the fitness of the simulation of the  $X_{Ps}$  did not improve (Figure 6.2B) when  $k_{BAC}$  was set to  $2.57 \times 10^{-10}$   $\mu$ mole/hr-cell and  $Y_{BAC}$  was  $1.43 \times 10^9$  cell/ $\mu$ mole BAC.

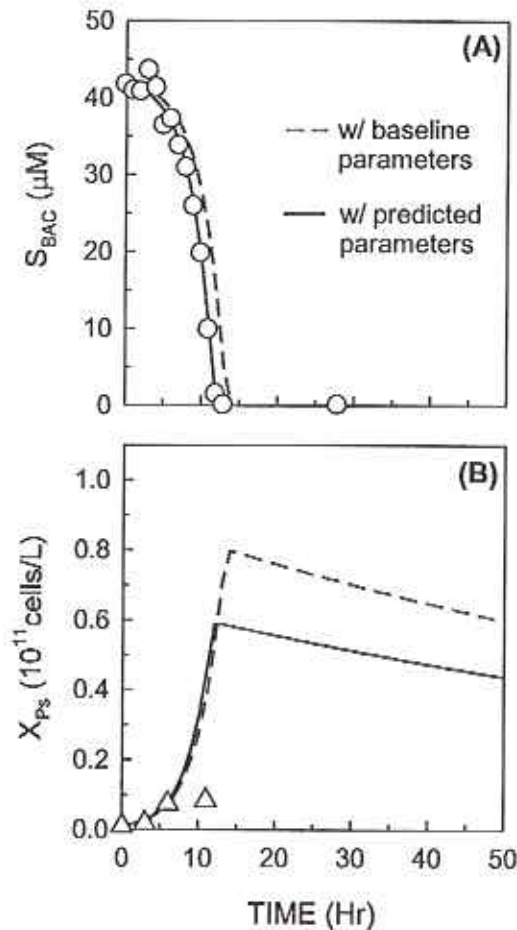


Figure 6.2. Profile of (A) BAC degradation and (B) BIOMIG1 growth in a batch reactor. Lines represent model simulations with different set of parameter values.

### 6.2.2. Maltose Degradation in Batch Reactors by *E. coli*

A batch reactor was operated for 30 hours and *E. coli* density was measured by optical density and plate counting throughout the experiment. The initial maltose concentration in the reactor was 2921  $\mu\text{M}$  and *E. coli* density was  $8.4 \times 10^8$  cells/L. The *E. coli* density peaked up within 10 hours and reached to  $1 \times 10^{12}$  cells/L at the end of the 30 hours (Figure 6.3). The fit of the model simulations with baseline parameter values (Table 5.4) had an  $R^2$  equal to 0.98 (Figure 6.3). The parameters  $k_{\text{Malt}}$  and  $Y_{\text{Malt}}$  were predicted by fitting the model to the experimental data. The model predictions improved and the  $R^2$  value has increased to 0.99 when  $k_{\text{Malt}}$  was  $6.6 \times 10^{-10}$   $\mu\text{mole/hr-cell}$  and  $Y_{\text{Malt}}$  was  $5.25 \times 10^8$  cell/ $\mu\text{mole}$  Maltose (Figure 6.3).

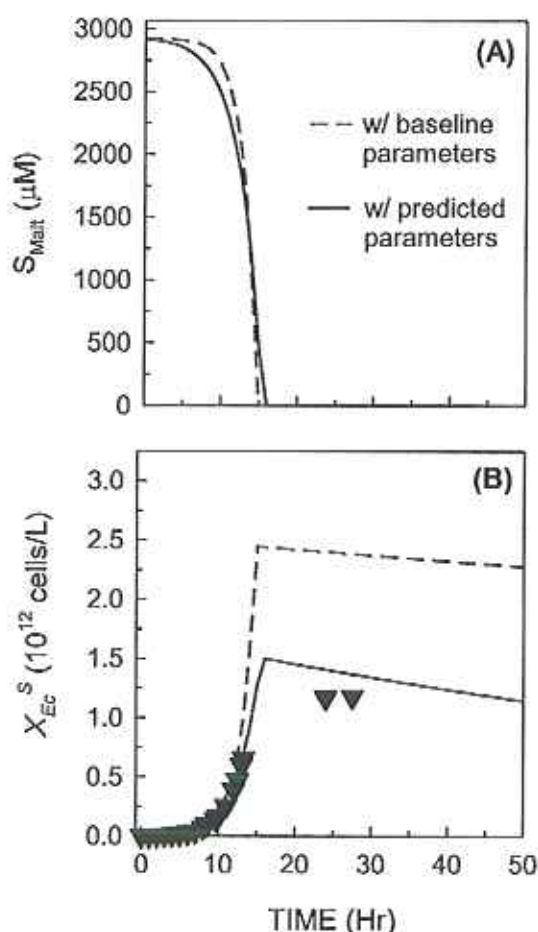


Figure 6.3. Profile of (A) maltose degradation and (B) *E. coli* growth in a batch reactor. Lines represent model simulations with different set of parameter values.

### 6.2.3. Growth Dynamics of the Co-culture Batch Reactor Under BAC Stress

A batch reactor was operated for approximately 90 hours. *E. coli* growth was recorded with optical density measurements and plate counting throughout the experiment. The initial maltose concentration while the BAC concentration was approximately 42  $\mu\text{M}$ . The initial *E. coli* concentration was  $1.4 \times 10^9$  cells/L and the BIOMIG1 concentration was  $6.8 \times 10^9$  cells/L in the reactor. The  $k_{\text{BAC}}$  was set at  $2.57 \times 10^{-10}$   $\mu\text{mole/hr-cell}$  and  $k_{\text{Malt}}$  was set at  $6.6 \times 10^{-10}$   $\mu\text{mole/hr-cell}$  while  $Y_{\text{BAC}}$  was fixed to  $1.43 \times 10^9$  cell/ $\mu\text{mole BAC}$  and while  $Y_{\text{Malt}}$  was fixed to  $5.25 \times 10^8$  cell/ $\mu\text{mole Maltose}$ . The parameter values were extracted from the previously predicted data obtained from fitting the model to the mono-culture batch experimental data. Within 15 hours, the BAC concentration approached to 0 (Figure 6.4A) and the BIOMIG1 density reached to its peak of  $8.4 \times 10^9$  cells/L (Figure 6.4B). The  $R^2$  for the BAC degradation simulation was found to be 0.98 while it failed to simulate the BIOMIG1 growth with an  $R^2$  value of 0.60.

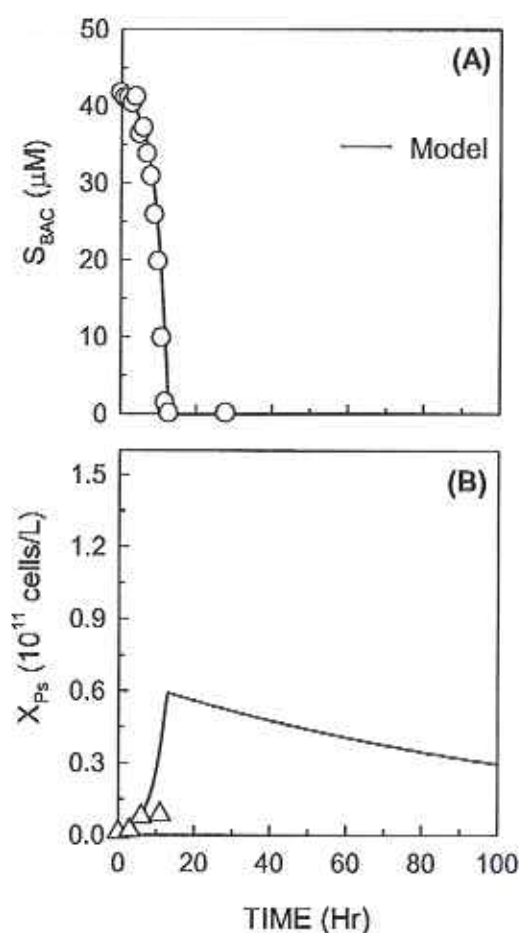


Figure 6.4. Profile of (A) BAC utilization and (B) BIOMIG1 growth in the co-culture batch reactor. Solid line represents model simulations of the variables  $S_{BAC}$  and  $X_{Ps}$ .

Meanwhile the susceptible *E. coli* density reached to its peak of  $9.5 \times 10^{11}$  cells/L in 75 hours. The  $UP$  and  $Enh$  constants were predicted by fitting the experimental *E. coli* growth data to the model and found to be  $22 \mu\text{M}$  and  $1.407$  respectively as given in Table 6.1. According to this, within the window of  $22 \mu\text{M}$  and  $43 \mu\text{M}$ , the negative inhibition effect of BAC on susceptible *E. coli* growth continues by amplifying the decay by taking its exponent power of 1.37. With these predicted values, the  $R^2$  for the *E. coli* growth was calculated as 0.99. Contrary to this, growth of resistant *E. coli* wasn't observed at all even though it is predicted by the model. This was mainly due to the low concentration of the resistant *E. coli* and the limitations of the plating technique.

Table 6.1. Fixed parameters of the batch co-culture *E. coli* and BIOMIG1 experiment.

Parameter	Value
Initial BAC ( $\mu\text{M}$ )	41.6
Initial Maltose ( $\mu\text{M}$ )	2921
$X_{Ps}$ (cell/L)	$6.81 \times 10^9$
$X_{Ec}$ (cell/L)	$1.41 \times 10^9$
D ( $\text{hour}^{-1}$ )	0
$k_{BAC}$ ( $\mu\text{mol/hr} \cdot \text{cell}$ )	$2.57 \times 10^{-10}$
$k_{Malt}$ ( $\mu\text{mol/hr} \cdot \text{cell}$ )	$6.6 \times 10^{-10}$
$M_{BAC}$ ( $\mu\text{M}$ )	1
$M_{Malt}$ ( $\mu\text{M}$ )	1.13
$Y_{Malt}$ (cell/ $\mu\text{M } S_{Malt}$ )	$5.25 \times 10^8$
$Y_{BAC}$ (cell/ $\mu\text{M } S_{BAC}$ )	$1.43 \times 10^9$
$k_d$ ( $\text{hour}^{-1}$ )	$2.08 \times 10^{-3}$
MIC ( $\mu\text{M}$ )	43
UP ( $\mu\text{M}$ )	22
LOW ( $\mu\text{M}$ )	10
P	$10^{-6}$
Enh	1.407

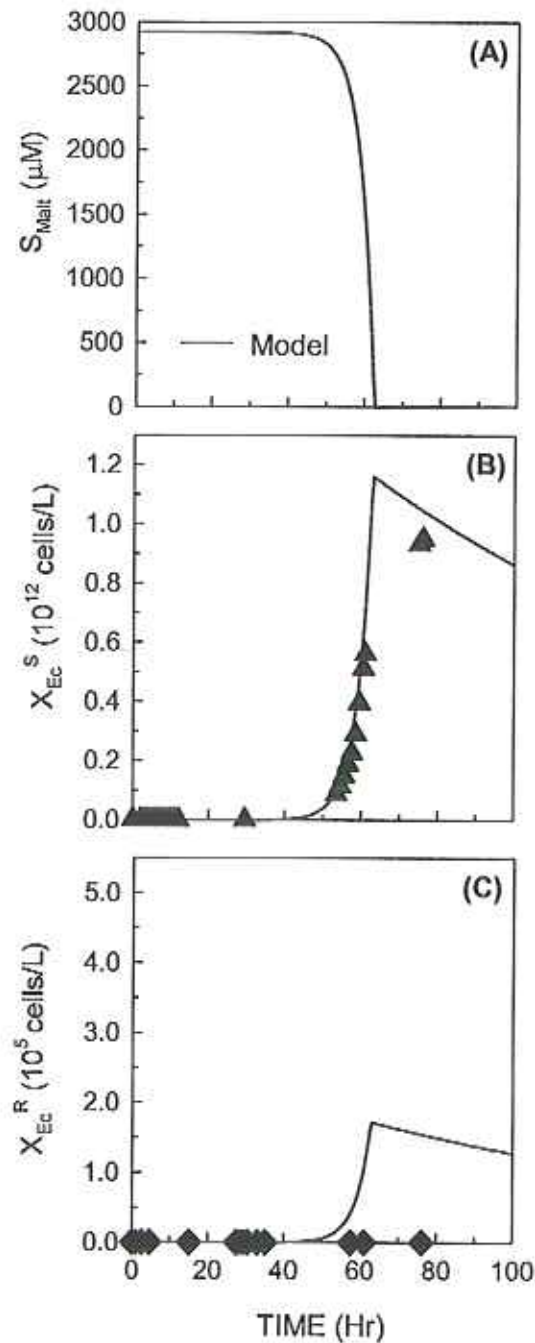


Figure 6.5. Profile of (A) predicted maltose utilization, (B) susceptible and (C) resistant *E. coli* growth in the co-culture batch reactor. Solid line represents model simulations of the variables  $S_{\text{Malt}}$  and  $X_{\text{Ec}}^{\text{S}}$  and  $X_{\text{Ec}}^{\text{R}}$ .

### 6.3. Model Verification and Simulations

Model verification was performed with the data obtained from continuous flow reactor system. The dilution rate was set at  $0.10 \text{ hour}^{-1}$  which resulted in a flow rate of  $0.86 \text{ ml/min}$ . The experiment lasted 196 hours and data were collected daily. The reactor contained  $2921 \mu\text{M}$  maltose and  $43 \mu\text{M}$  BAC while it was fed with M9 media containing same amount of maltose and BAC. The

initial *E. coli* concentration was  $1.41 \times 10^9$  cells/L and the initial BIOMIG1 concentration was  $4.78 \times 10^8$  cells/L while the bacteria concentration of the feed were 0 and controlled throughout the experiment. The parameter values were set as predicted from the batch experiments;  $k_{BAC}$  and  $k_{Malt}$  was fixed at  $2.57 \times 10^{10}$  and  $6.6 \times 10^{-10}$   $\mu\text{mol/hr-cell}$  and  $Y_{BAC}$  and  $Y_{Malt}$  was fixed at  $1.43 \times 10^9$  cell/ $\mu\text{M } S_{BAC}$  and  $5.25 \times 10^8$  cell/ $\mu\text{M } S_{Malt}$ . Lastly,  $Up$  was set at 22  $\mu\text{M}$  and  $Enh$  was set at 1.307. All the BAC in the system were degraded within 40 hours and the model prediction of BAC degradation yielded an  $R^2$  value of 0.73 and was in accordance with the experimental data (Figure 6.6A). Even though the peak of the BIOMIG1 concentration was found to be approximately  $6.0 \times 10^{10}$  the model failed to simulate this rise with an  $R^2$  value of 0.60. Despite this, the model prediction of the concentration at which a stability has been reached was in accordance with the experimental data.

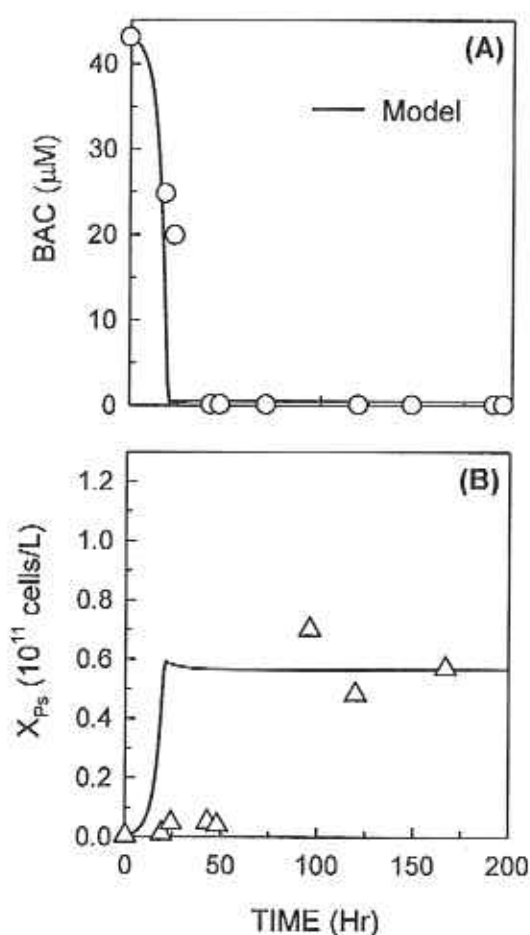


Figure 6.6. Profile of (A) BAC utilization and (B) BIOMIG1 growth in a continuous flow reactor. Solid line represents model simulations of the variables  $S_{BAC}$  and  $X_{Ps}$ .

Meanwhile, the growth of susceptible *E. coli* has reached a maximum of  $1.0 \times 10^{12}$  cells/L within 125 hours (Figure 6.7B). The  $R^2$  value between the model prediction and the experimental

values was found to be 0.98. Additionally, experimental results yielded resistant *E. coli* starting from 100<sup>th</sup> hour with a maximum concentration of  $6 \times 10^5$  cells/L. (Figure 6.7C). The *P* and *LOW* constant were fitted to this resistant *E. coli* growth data although the initial fitness wasn't bad. The *P* value was predicted as  $1.6 \times 10^{-6}$  and the *LOW* value as  $7.2 \mu\text{M}$  (Table 6.2). With this new values, the goodness of fit rose and  $R^2$  has reached 0.99.

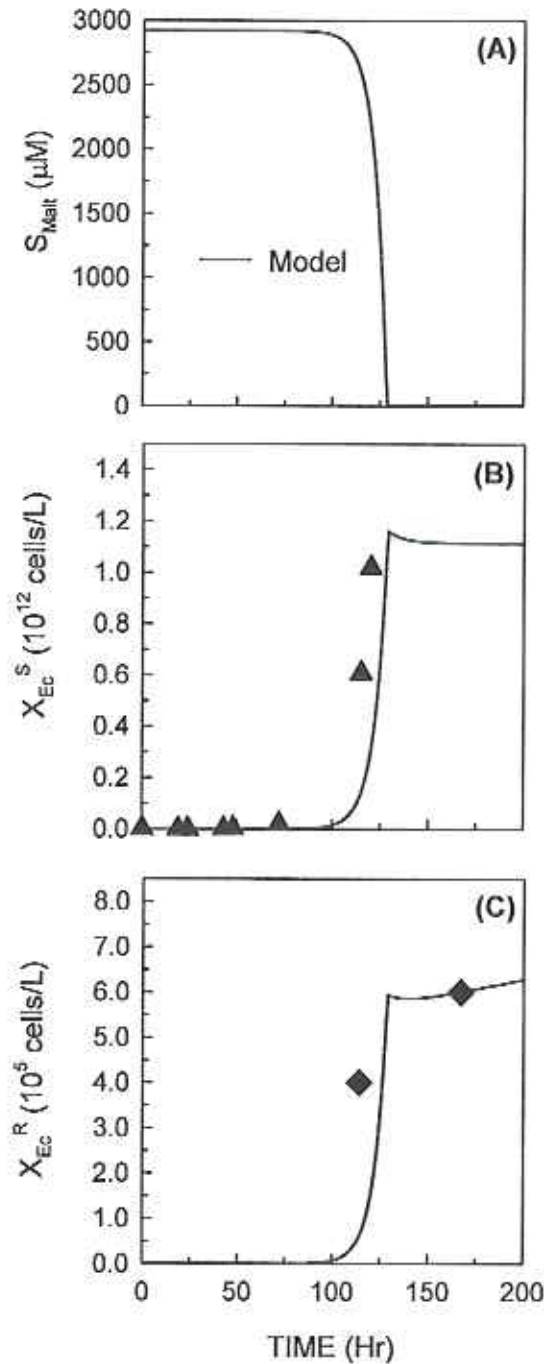


Figure 6.7. Profile of (A) predicted maltose utilization, (B) susceptible and (C) resistant *E. coli* growth in a continuous flow reactor. Solid line represents model simulations of the variables  $S_{\text{Malt}}$  and  $X_{\text{Ec}}^{\text{S}}$  and  $X_{\text{Ec}}^{\text{R}}$ .

Table 6.2. Fixed parameters of the continuous co-culture *E. coli* and BIOMIG1 experiment.

Parameter	Value
Initial BAC ( $\mu\text{M}$ )	43
Initial Maltose ( $\mu\text{M}$ )	2921
$X_{Ps}$ (cell/L)	$4.78 \times 10^8$
$X_{Ec}$ (cell/L)	$1.41 \times 10^9$
D ( $\text{hour}^{-1}$ )	0.10
$k_{BAC}$ ( $\mu\text{mol/hr} \cdot \text{cell}$ )	$2.57 \times 10^{-10}$
$k_{Malt}$ ( $\mu\text{mol/hr} \cdot \text{cell}$ )	$6.6 \times 10^{-10}$
$M_{BAC}$ ( $\mu\text{M}$ )	1
$M_{Malt}$ ( $\mu\text{M}$ )	1.13
$Y_{Malt}$ (cell/ $\mu\text{M } S_{Malt}$ )	$5.25 \times 10^8$
$Y_{BAC}$ (cell/ $\mu\text{M } S_{BAC}$ )	$1.43 \times 10^9$
$k_d$ ( $\text{hour}^{-1}$ )	$2.08 \times 10^{-3}$
MIC ( $\mu\text{M}$ )	43
UP ( $\mu\text{M}$ )	22
LOW ( $\mu\text{M}$ )	7.3
P	$1.6 \times 10^{-6}$
Enh	1.407

#### 6.4. Simulations to Identify the Resistance Promoting Conditions

By fitting the parameters to the experimental data, the sensitivity of the model has been increased. With this, various simulations were conducted to deduce the occurrence of *E. coli*<sup>Res</sup> and the wash out of *E. coli*<sup>Sus</sup> at different conditions.

The initial BAC concentration was one of the most restraining factors for the growth of *E. coli*<sup>Res</sup>. For this reason, the model was simulated in the same initial conditions of co-culture continuous experiment as in Table 6.2 with different BAC concentrations of 0, 4, 6, 16 and 32 mg/L and the growth of BIOMIG1, *E. coli*<sup>Sus</sup> and *E. coli*<sup>Res</sup> was plotted as in Figure 6.8.

*E. coli*<sup>Sus</sup> reached the same concentration at every concentration of BAC with different lag phases at each concentration. While it reaches a maximum of  $1.2 \times 10^{12}$  before the 50<sup>th</sup> hour when there is no BAC in the medium, it can only reach this maximum after the 150<sup>th</sup> hour when the BAC concentration is 32 mg/L.

*E. coli<sup>Res</sup>* reaches to different final concentrations at different BAC levels. While there isn't any resistant *E. coli* when the system isn't treated with any BAC, it reaches a peak of  $0.4 \times 10^7$  cells/L at the 40<sup>th</sup> hour and continues to rise when the BAC concentration is 4 mg/L both in the initial medium as well as in the feed. With increasing BAC concentration, both the maximum cell yield as well as the lag phase increases.

Contrary to this, the yield of BIOMIG1 increases with the BAC concentration in the medium feed and would probably continue to rise with increasing BAC concentrations.

The change in the dilution rate was simulated as well. The growth of *E. coli<sup>Sus</sup>* was inhibited and all the community in the medium was washed out with increasing dilution rates. At a rate of  $0.20 \text{ hour}^{-1}$  all *E. coli<sup>Sus</sup>* and *E. coli<sup>Res</sup>* were washed out from the system while BIOMIG1 remained in the system and reached approximately to the same maximum cell concentration at each dilution rate.

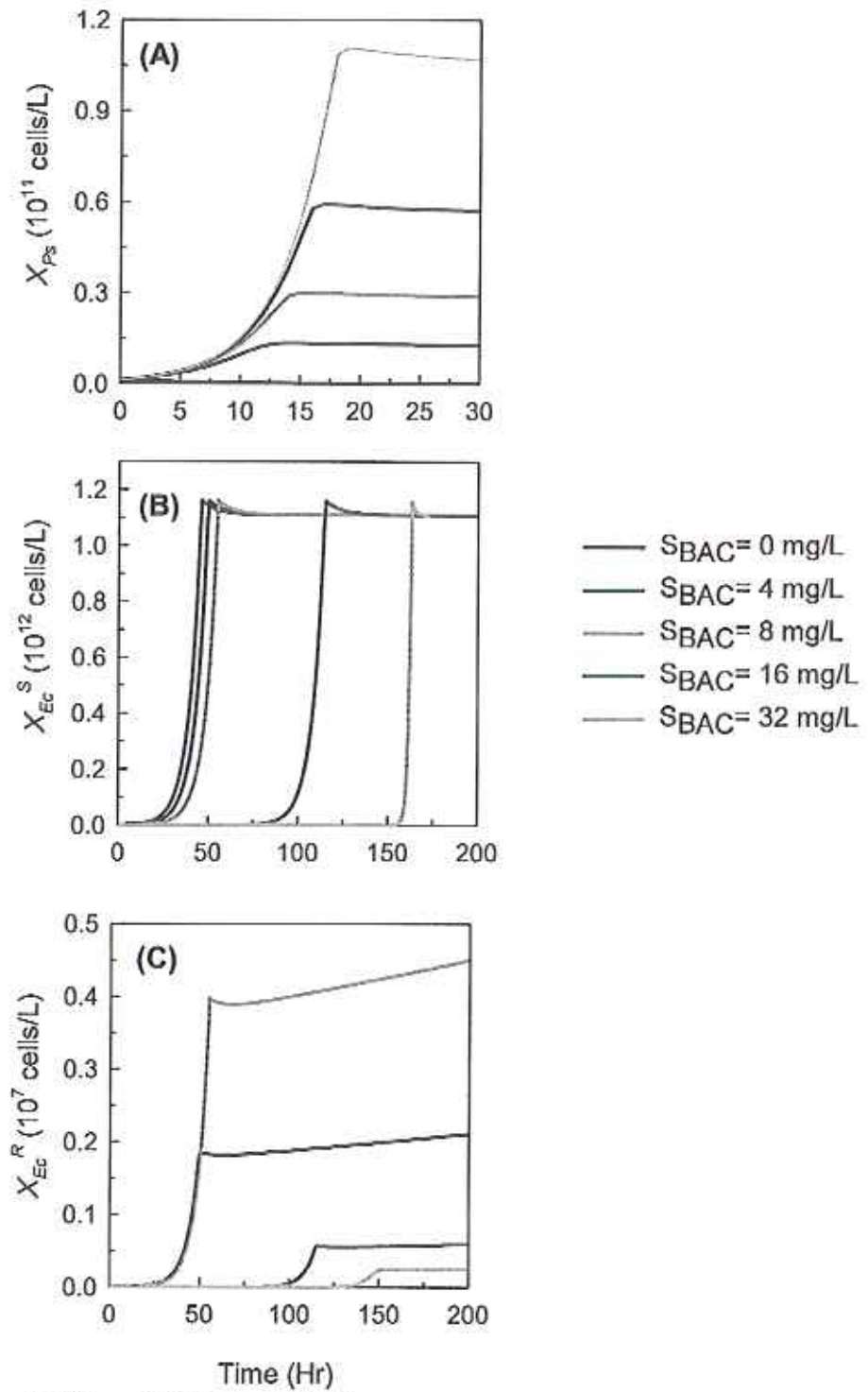


Figure 6.8. Simulations of different BAC concentrations.

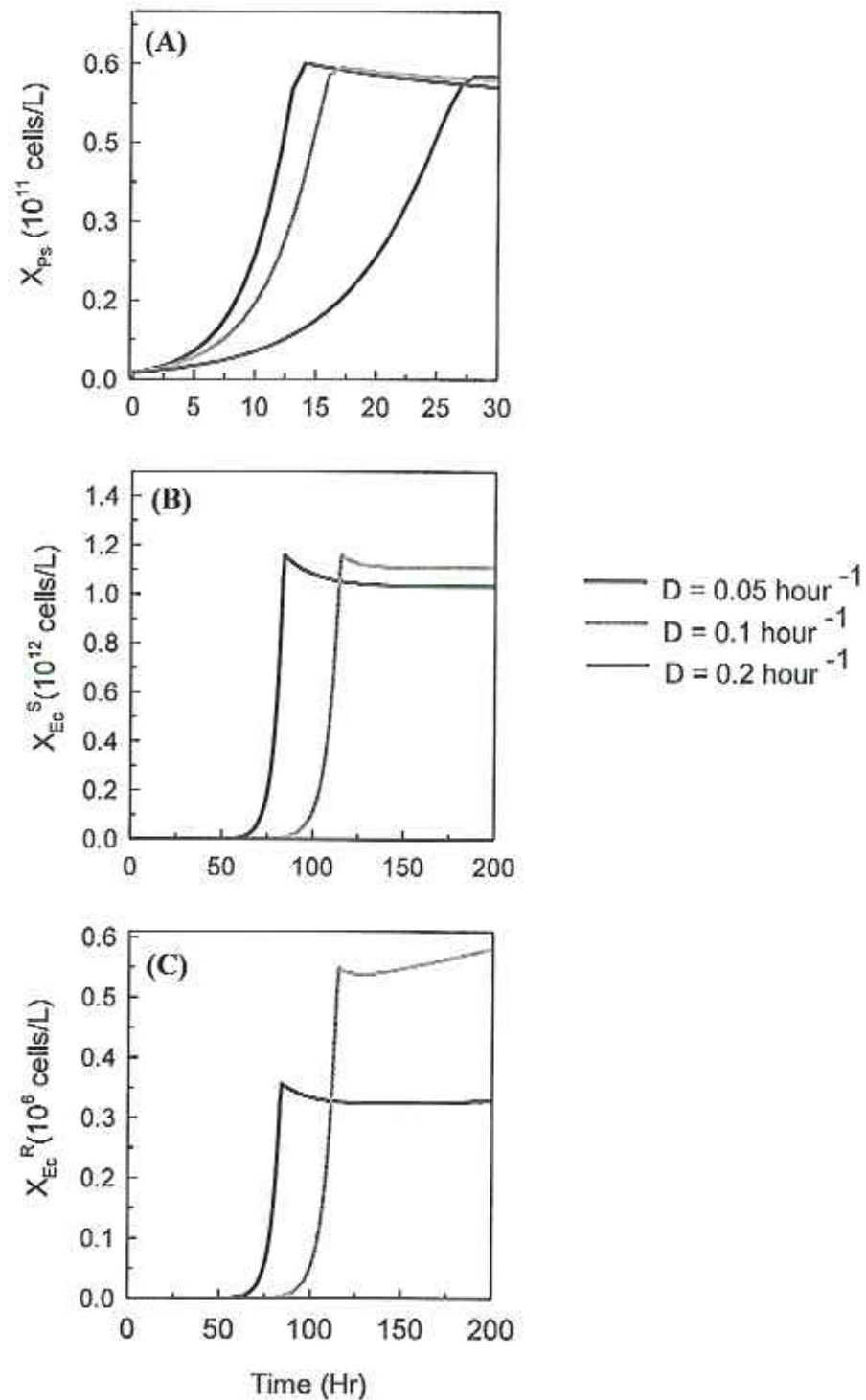


Figure 6.9. Simulations for different  $Q$  values.

Another point that aroused curiosity was on how the model would behave when BIOMIG1 is not present but BAC concentration is below the  $UP$  level. It is expected that resistant *E. coli* (*E. coli<sup>Res</sup>*) thrive regardless of the presence of a BAC degrader.

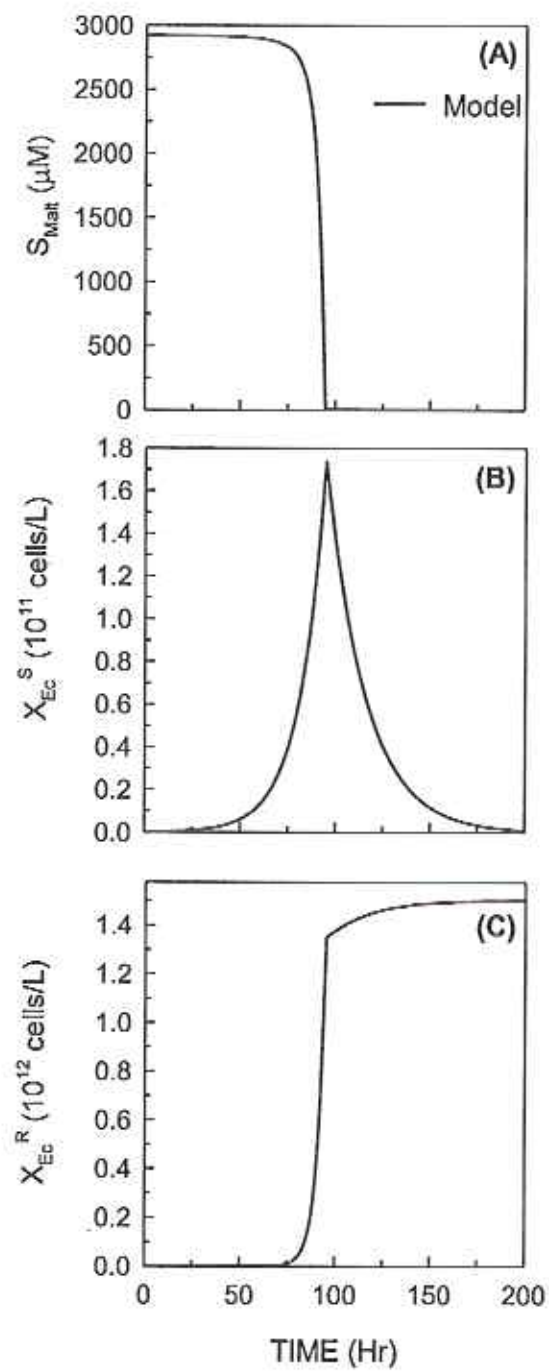


Figure 6.10. (A) Maltose concentration, (B) *E. coli Sus* concentration and (C) *E. coli Res* concentration when BAC is fixed at 21  $\mu\text{M}$  (8 mg/L) and the BIOMIG1 concentration is 0.

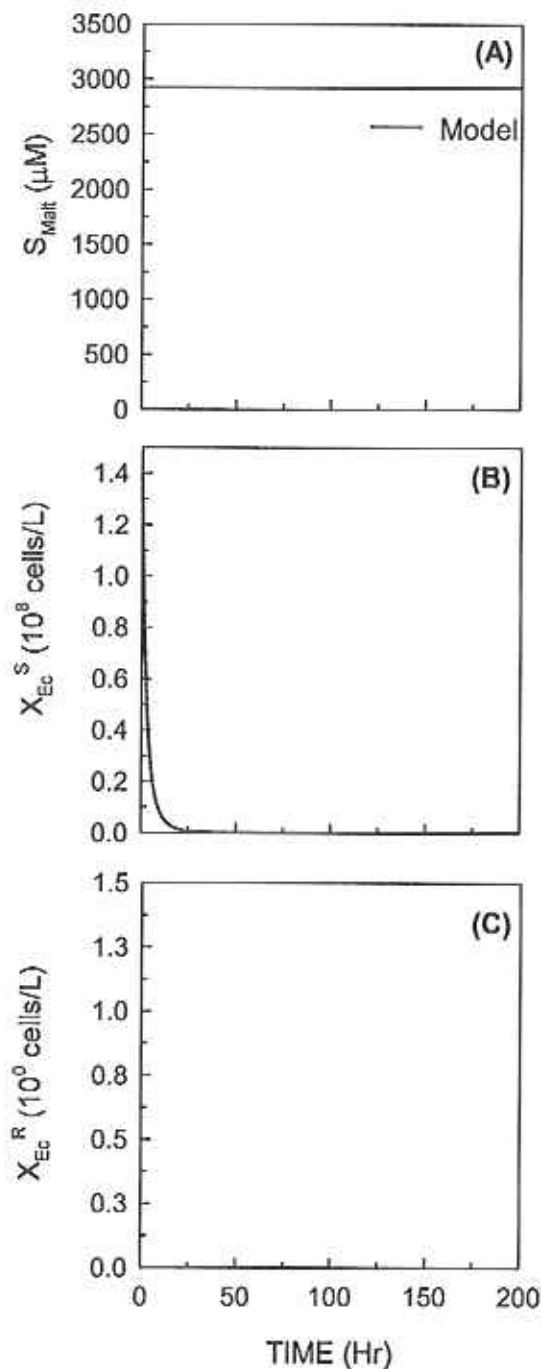


Figure 6.11. (A) Maltose concentration, (B) *E. coli*<sup>Sus</sup> concentration and (C) *E. coli*<sup>Res</sup> concentration when BAC is fixed at 43  $\mu\text{M}$  (8 mg/L) and the BIOMIG1 concentration is 0.

In Figure 6.10 the growth of *E. coli*<sup>Sus</sup> continues until a significant increase in the *E. coli*<sup>Res</sup> concentration. Then, the *E. coli*<sup>Sus</sup> is outcompeted by the *E. coli*<sup>Res</sup>. As a control, the same run was repeated at 43  $\mu\text{M}$  of BAC ( Figure 6.11) and it is observed that resistant *E. coli* does not occur at all while susceptible *E. coli* dies out rapidly.

Furthermore, the maltose concentration in Figure 6.11A does not change at all which is another indicator of the inhibition effect of BAC on susceptible *E. coli*. Overall, this makes sense as it was observed in the previous simulation (Figure 6.8) of different BAC concentrations that resistant *E. coli* blooms when the BAC concentration is closest to the *UP* level which was set as 8 mg/L in the model. This gives the *E. coli* an opportunity to develop resistance as it is still below the minimum inhibitory concentration, but nevertheless puts a selective pressure on the community.

## 7. CONCLUSIONS

Throughout this research, the effect of dynamically changing sub-inhibitory concentrations of BAC was tested in a continuous co-culture system. The recently isolated *Pseudomonas sp.* BIOMIG1 strain was used as the BAC degrader and *E. coli* was used as the susceptible microorganism. It was observed that the continuous BAC degradation of BIOMIG1 created a favorable environment for *E. coli* to survive at concentrations higher than its minimum inhibitory concentration. Furthermore, the continuous system resulted in an increase in the tolerance of *E. coli* to BAC. This was proved with growth on plates containing 256 mg/L BAC which was not possible without the continuous system.

In the second step of this research, the continuous co-culture system was modelled and the data obtained from the batch and continuous experiments were used to estimate the parameters in the model. Once all the parameters were predicted, the conditions in which resistant *E. coli* could be observed were determined. It has been found that a significant decrease in resistant *E. coli* growth occurs between 4 mg/L and 8 mg/L of BAC concentration. Moreover, the sensitivity of the susceptible and resistant *E. coli* to being washed out was tested and found out that 0.01 hour<sup>-1</sup> was a good estimate for resistant *E. coli* to grow as slower rates decreases the yield while higher rates causes a wash out in the susceptible *E. coli* itself.

The model developed was only meant to simplify the processes to better understand the further implications of biocide consumption in the presence of a degrader and not to determine the quantitative results of a reactor system. With it, the approximate relationship between the initial bacterial density and biocide concentration can further be explored. Furthermore, the results of a co-culture experiment can be reciprocated if the minimum inhibitory concentration of the community is known. This, itself, can facilitate the design of future experiments that need to be conducted to further elaborate the model. Nevertheless, this research and the model developed have two significances. Firstly, there are multiple examples of the effect of various antimicrobial agents on various microorganisms. But most examples in the literature are based on the effect of a fixed concentration of antimicrobial agent on a single microorganism. In this research, the effect of dynamically changing BAC concentration has been observed in a co-culture system. Here, both the dynamic change and the co-culture are relatively novel for this kind of research. Secondly, the literature on modeling resistance development in a co-culture continuous system is quite obscure and this research aims to contribute to this and expand the field.

The uncontrolled usage of biocides in hospital environments is still a common practice even though the correlation between antibiotic resistance and biocide resistance has been established for a long time. Therefore, it is important to broaden current scientific knowledge on the transformation a microbial community experiences in an extensively polluted environment, such as on hospital surfaces. This research, with its focus on BIOMIG1, tries to contribute to the literature on biocide resistance in polluted surfaces though it has many shortcomings which can be improved by further research. Among these, the exploration of a more complex and heterogeneous environment has vital importance as this is the case in the real world. Additionally, the model can be developed further to estimate what happens at dynamically sustained biocide selection where biocide concentration is increased with increasing resistance. With this, adaptive pathways to higher levels of resistance can be explored as recommended by Toprak et al. in their publication on the effects of adjusted antibiotic concentration on resistance evolution (Toprak, et al. 2011).

## REFERENCES

- Aiello, A. E., Larson, E., 2003. Antibacterial cleaning and hygiene products as an emerging risk factor for antibiotic resistance in the community. *Infectious Diseases*, 3, 501-506.
- Akimitsu, N., Hamamoto, II., Inoue, R., 1999. Increase in resistance of methicillin-resistant staphylococcus aureus to  $\beta$ -lactams caused by mutations conferring resistance to benzalkonium chloride, a disinfectant widely used in hospitals. *Antimicrobial Agents and Chemotherapy*, 43, 3042-3043.
- Alekshun, M., Levy, S. B., 2007. Molecular mechanisms of antibacterial multidrug resistance. *Cell*, 128, 1037-1050.
- Allen, H. K., Donato, J. Wang, H. H., Cloud-Hansen, K., Davies, J., Handelsman, J., 2010. Call of the wild: antibiotic resistance genes in natural environments. *Nature Reviews*, 8, 251-259.
- Anthonisen, I. -L., Sunde, M., Steinum, T. M., Sidhu, M. S., Sørum, H., 2002. Organization of the antiseptic resistance gene *qacA* and Tn552-related beta-lactamase genes in multidrug-resistant *Staphylococcus haemolyticus* strains of animal and human origins. *Antimicrobial Agents and Chemotherapy*, 46, 3606-3612.
- Baquero, F., Martínez, J.-L., Cantón, R., 2008. Antibiotics and antibiotic resistance in water environments. *Current Opinion in Biotechnology*, 19, 260-265.
- Blair, Jessica M. A., Webber, M. A., Baylay, A. J., Ogbolu, D. O., and Piddock, L. J. V., Molecular mechanisms of antibiotic resistance. *Nature Reviews Microbiology*, 13, 42-51.
- Cantón, R., Morosini, M.-I., 2011. Emergence and spread of antibiotic resistance following exposure to antibiotics. 35, 977-991.
- Carmona-Ribeiro, A. M., Dias de Melo Carrasco, L., 2013. Cationic antimicrobial polymers and their assemblies. *International Journal of Molecular Sciences*, 14, 9906-9946.

Carmona-Ribeiro, A. M., Vieira, D. B. , Lincopan, N., 2006. Cationic surfactants and lipids as anti-infective agents. *Anti-Infective Agents in Medicinal Chemistry*, 5, 33-54.

Clara, M., Scharf, S., Scheffknecht, C. , Gans, O., 2007. Occurrence of selected surfactants in untreated and treated sewage. *Water Research*, 41, 4339-4348.

Cloete, T., 2003. Resistance mechanisms of bacteria to antimicrobial compounds. *International Biodeterioration and Biodegradation*, 51, 277-282.

Contois, D. E., 1959. Kinetics of bacterial growth: relationship between population density and specific growth rate of continuous cultures. *Journal of General Microbiology*, 21, 40-50.

Cookson, B., 2005. Clinical significance of emergence of bacterial antimicrobial resistance in the hospital environment. *Journal of Applied Microbiology*, 99, 989-996.

Ertekin, E., 2017. Microbial ecology and genetics of benzalkonium chloride biotransformation in the environment, Ph.D. Thesis, Boğaziçi University, Turkey.

Ertekin, E., Hatt, J. K., Konstantinidis, K. T. , Tezel, U., 2016. Similar microbial consortia and genes are involved in the biodegradation of benzalkonium chlorides in different environments. *Environmental Science and Technology*, 50, 4304-4313.

Fernandez, L., Breidenstein, E. B. M. , Hancock, R. E. W., 2012. Importance of adaptive and stepwise changes in the rise and spread of antimicrobial resistance. In: Keen, P. L., Montforts, M. H. M. M. (Eds), *Antimicrobial Resistance in the Environment*, 43-72. John Wiley and Sons, Inc., New Jersey, U.S.A.

Focks, A., 2005. Modeling the transfer of antibiotic drug resistance genes between E.coli-strains. B.Sc. Thesis, University of Osnabrueck, Germany.

Gül, G., 2013. Antibiotic resistant *Pseudomonas* Sp. BIOMIG1 protects susceptible bacteria from disinfectants, M.Sc. Thesis, Boğaziçi University, Turkey.

Gauld, K., 2016. Antibiotics: from prehistory to the present day. *Journal of Antimicrobial Chemotherapy*, 71, 572-575.

- Gerba, C. P., 2015. Quaternary ammonium biocides: efficacy in application. *Applied and Environmental Microbiology*, 81, 464-469.
- Gilbert, P., Al-Taae, A. N. A., 1985. Antimicrobial activity of some alkyl-trimethyl ammonium bromides. *Letters of Applied Microbiology*, 1, 101-105.
- Gilbert, P., McBain, A., 2003. Potential impact of increased use of biocides in consumer products on prevalence of antibiotic resistance. *Clinical Microbiology Reviews*, 16, 189-208.
- Gullberg, E. et al., 2011. Selection of resistant bacteria at very low antibiotic concentrations. *PLoS Pathogens*, 7, 1-9.
- Hegstad, K. et al., 2010. Does the wide use of quaternary ammonium compounds enhance the selection and spread of antimicrobial resistance and thus threaten our health?. *Microbial Drug Resistance*, 16, 91-104.
- Hellweger, F. L., Ruan, X., Sanchez, S., 2011. A simple model of tetracycline antibiotic resistance in the aquatic environment (with application to the Poudre river). *International Journal of Environmental Research and Public Health*, 8, 480-497.
- Hermesen, R., Deris, J. B., Hwa, T., 2012. On the rapidity of antibiotic resistance evolution facilitated by a concentration gradient. *PNAS*, 109, 10775-10780.
- Ibargüen-Mondragón, E., Mosquer, S., Cerón, M., Burbano-Rosero, E. M., Hidalgo-Bonilla, S. P., Esteva, L., Romcro-Leitón, J. P., 2014. Mathematical modeling on bacterial resistance to multiple antibiotics caused by spontaneous mutations. *BioSystems*, 117, 60-67.
- Kümmerer, K., Eitel, A., Braum, U., Hübner, P., Daschner, F., Mascart, G., Milandri, M., Reinthaler, F., Verhoef, J., 1997. Analysis of benzalkonium chloride in the effluent from European hospitals by solid-phase extraction and high-performance liquid chromatography with post-column ion-pairing and fluorescence detection. *Journal of Chromatography A*, 774, 281-286.
- Kohanski, M. A., Dwyer, D. J., Collins, J. J., 2010. How antibiotics kill bacteria: from targets to networks. *Nature Reviews Microbiology*, 8, 423-435.

Kummerer, K., 2004. Resistance in the environment. *Journal of Antimicrobial Chemotherapy*, June, 54, 311-320.

Levin, B. R., Udekwi, K. I., 2010. Population dynamics of antibiotic treatment: a mathematical model and hypotheses for time-kill and continuous-culture experiments. *Antimicrobial Agents and Chemotherapy*, 54, 3414-3426.

Levy, S. B., 2000. Antibiotic and antiseptic resistance: impact on public health. *Pediatric Infectious Diseases*, 19, 120-122.

Madigan, M. T., Martinko, J. M., Parker, J., 2003. *Brock biology of microorganisms*. Prentice Hall, Pearson Education Inc. San Francisco, U.S.A.

Maillard, J. -Y., 2002. Bacterial target sites for biocide action. *Journal of Applied Microbiology Symposium Supplement*, 92, 16-S-27-S.

Martinez, J.-L., Olivares, J., 2012. Environmental pollution by antibiotic resistance genes. In: Keen, P. L., Montforts, M. H. M. M. (Eds), *Antimicrobial Resistance in the Environment*, 151-172, John Wiley and Sons, Inc., New Jersey, U.S.A.

McBain, A. J., Ledger, R. G., Moore, L. E., Catrenich, C. E., Gilbert, P., 2004. Effects of quaternary-ammonium-based formulations on bacterial community dynamics and antimicrobial susceptibility. *Applied and Environmental Microbiology*, 70, 3449-3456.

McDonnell, G., Russell, A. D., 1999. Antiseptic and disinfectants: activity, action, and resistance. *Clinical Microbiology Reviews*, 12, 147-179.

McKenna, S. M., Davies, K. J. A., 1988. The inhibition of bacterial growth by hypochlorous acid. *Biochemistry Journal*, 254, 685-692.

Miao, V., Davies, D., Davies, J., 2012. Path to resistance. In: Keen, P. L., Montforts, M. H. M. M. (Eds), *Antimicrobial Resistance in the Environment*, 7-15, John Wiley and Sons, Inc., New Jersey, U.S.A.

Negri, M.-C., Lipsitch, M., Blázquez, J., Levin, B. B., Baquero, F., 2000. Concentration-dependent selection of small phenotypic differences in TEM beta-lactamase-mediated antibiotic resistance. *Antimicrobial Agents and Chemotherapy*, 44, 2485-2491.

Okpokwasili, G. C. , Nwcke, C. O., 2005. Microbial growth and substrate utilization kinetics. *Journal of Biotechnology*, 5, 305-317.

Opatowski, I., Guillemot, D., Boëlle, P.-Y., Termime, L., Contribution of mathematical modeling to the fight against bacterial antibiotic resistance. *Current Opinion in Infectious Diseases*, 24, 279-287.

Pryor, A. K., Brown, R. S., 1975. Quaternary ammonium disinfectants. *Journal of Environmental Health*, 37, 326-330.

Rittmann, B. E., McCarty, P. L., 2001. *Environmental biotechnology: principles and applications*. McGraw Hill, New York, U.S.A

Roberts, M. C., 2012. Mechanisms of bacterial antibiotic resistance and lessons learned from the environmental tetracycline-resistant bacteria. In: Keen, P. L., Montforts, M. H. M. M. (Eds), *Antimicrobial Resistance in the Environment*, 93-122, John Wiley and Sons, Inc., New Jersey, U.S.A.

Russell, A. D., 2002a. Introduction of biocides into clinical practice and the impact on antibiotic-resistant bacteria. *Journal of Applied Microbiology Symposium Supplement*, 92, 121S-135S.

Russell, A. D., 2002b. Antibiotic and biocide resistance in bacteria: Introduction. *Journal of Applied Microbiology Symposium Supplement*, 92, 1S-3S.

Russell, A. D., 2003. Biocide use and antibiotic resistance: the relevance of laboratory findings to clinical and environmental situations. *Infectious Diseases*, 3, 794-803.

SCENIHR (Scientific Committee on Emerging and Newly Identified Health Risks), 2009. *Assessment of the Antibiotic Resistance Effects of Biocides*, Brussels, Belgium.

Sidhu, M. S., Sørum, H., Holck, A., 2002. Resistance to quaternary ammonium compounds in food-related bacteria. *Microbial Drug Resistance*, 8, 393-9.

Tezel, U., Pavlostathis, S. G., 2011. Role of quaternary ammonium compounds on antimicrobial resistance in the environment. In: Keen, P. L., Montforts, M. H. M. M. (Eds), *Antimicrobial Resistance in the Environment*, 349-387, John Wiley and Sons, Inc., New Jersey, U.S.A.

Tezel, U., Pavlostathis, S. G., 2015. Quaternary ammonium disinfectants: microbial adaptation, degradation and ecology. *Current Opinion in Biotechnology*, 33, 296-304.

Toprak, E., Adrian V., Jean-Baptiste M., Remy C., Daniel L. H., and Roy K., 2011. Evolutionary paths to antibiotic resistance under dynamically sustained drug selection. *Nature Genetics*, 44, 101-105.

Ventola, C. L., 2015. The antibiotic resistance crisis. *Pharmacy and Therapeutics*, 40, 277-283.

Wales, A. D., Davies, R. H., 2015. Co-selection of resistance to antibiotics, biocides and heavy metals, and its relevance to foodborne pathogens. *Antibiotics*, 4, 567-604.

Wright, G. D., 2012. Antibiotic resistome: A framework linking the clinic and the environment. In: Keen, P. L., Montforts, M. H. M. M. (Eds), *Antimicrobial Resistance in the Environment*, 15-28, John Wiley and Sons, Inc., New Jersey, U.S.A.

Yilmaz, F. Ö., Evaluation of factors affecting the biotransformation of Benzalkonium Chlorides by *Pseudomonas spp.*, M.Sc. Thesis, Boğaziçi University, Turkey.

Zwietering, M. H., Jongenburger, I., Rombouts, F. M., Riet, K. V., 1990. Modeling of bacterial growth curve. *Applied and Environmental Microbiology*, 56, 1875-1881.

## APPENDIX: THE CALIBRATED AND VERIFIED MODEL CODE

METHOD RK4

STARTTIME = 0

STOPTIME = 200

DT = 0.0005

; SUBSTRATE DEGRADATION

$$d/dt (S\_BAC) = Q/V * S\_BAC0 - Q/V * S\_BAC - (k\_BAC * S\_BAC * X\_PS) / (M\_BAC + S\_BAC)$$

$$Inh = IF S\_BAC >= UP THEN 0 ELSE (1 - S\_BAC / MIC)$$

$$d/dt (S\_Malt) = Q/V * S\_Malt0 - Q/V * S\_Malt - ((k\_Malt * S\_Malt * X\_EC) / (M\_Malt + S\_Malt)) * Inh - (k\_Malt * S\_Malt * X\_ECR) / (M\_Malt + S\_Malt)$$

; GROWTH OF MICROORGANISMS

$$d/dt (X\_PS) = Q/V * X\_PS0 - Q/V * X\_PS + Y\_BAC * (k\_BAC * S\_BAC * X\_PS) / (M\_BAC + S\_BAC) - k\_d * X\_PS$$

$$Rec = IF S\_BAC <= MIC THEN Dead ELSE (S\_BAC / MIC)$$

$$Dead = IF S\_BAC <= UP THEN 1 ELSE Enh$$

$$Trans = IF S\_BAC <= UP AND S\_BAC >= LOW THEN RANDOM(0, P) ELSE 0$$

$$d/dt (X\_EC) = Q/V * X\_EC0 - Q/V * X\_EC + (1 - Trans) * Y\_MALT * ((k\_Malt * S\_Malt * X\_EC) / (M\_Malt + S\_Malt)) * (Inh) - (k\_d * X\_EC) ^ (Rec)$$

$$d/dt (X\_ECR) = Q/V * X\_ECR0 - Q/V * X\_ECR + Y\_MALT * (k\_Malt * S\_Malt * X\_ECR) / (M\_Malt + S\_Malt) - k\_d * X\_ECR + Trans * Y\_MALT * (k\_Malt * S\_Malt * X\_EC) / (M\_Malt + S\_Malt) * Inh$$

; INITIAL VALUES

init X\_EC = 1.41\*10<sup>8</sup>

init X\_ECR = 0

init X\_PS = 1.2\*10<sup>9</sup>

init S\_BAC = 43

init S\_Malt = 2921

; REACTOR SETTINGS

X\_EC0 = 0

X\_ECR0 = 0

X\_PS0 = 0

S\_BAC0 = 43

S\_Malt0 = 2921

Q = 10

V = 100

; CONSTANTS

k\_BAC = 2.57\*10<sup>-10</sup>

k\_Malt = 6.6\*10<sup>-10</sup>

M\_Malt = 1

M\_BAC = 1.13

k\_d = 2.08\*10<sup>-3</sup>

Y\_MALT = 5.25\*10<sup>8</sup>

Y\_BAC = 1.43\*10<sup>9</sup>

MIC = 43

UP = 22

LOW = 7.3

P = 1.6\*10<sup>-6</sup>

Enh = 1.407